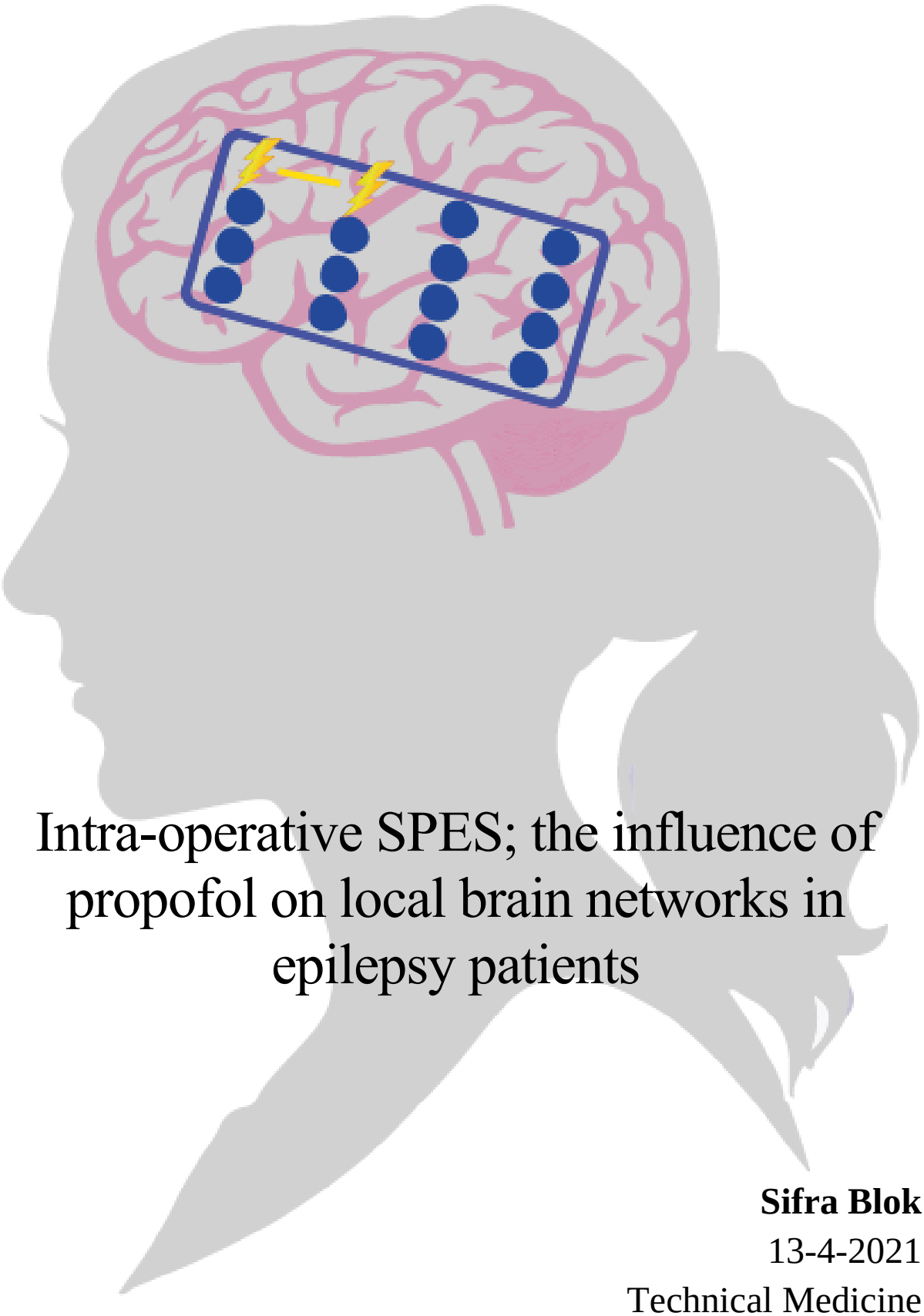

# Intra-operative SPES; the influence of propofol on local brain networks in epilepsy patients

**Sifra Blok**

13-4-2021

Technical Medicine

Final-version

# Intra-operative SPES; the influence of propofol on local brain networks in epilepsy patients

| | |
|---|---|
| Chairman | **Prof. dr. C. Brune**<br>University of Twente<br>Faculty of Electrical Engineering, Mathematics and Computer Science (EEMCS), Applied Analysis (AA) |
| Daily Supervisor | **D. van Blooijs MSc.**<br>University Medical Centre Utrecht<br>Department of Functional Neurosurgery and Epilepsy |
| Technical Supervisor (UT) | **Dr. H.G.E. Meijer**<br>University of Twente<br>Faculty of Electrical Engineering, Mathematics and Computer Science (EEMCS), Applied Analysis (AA) |
| Medical Supervisor | **Dr. F.S.S. Leijten**<br>University Medical Centre Utrecht<br>Department of Functional Neurosurgery and Epilepsy |
| Technical Supervisor (UMCU) | **Dr. G.J.M. Huiskamp**<br>University Medical Centre Utrecht<br>Department of Functional Neurosurgery and Epilepsy |
| Mentor | **Drs. B.J.C.C. Hessink-Sweep**<br>University of Twente<br>Faculty of Science and Technology (TNW), Technical Medicine (TG) |
| External Member | **M.M.L.H. Verhulst MSc.**<br>University of Twente<br>Faculty of Science and Technology (TNW), Clinical Neurophysiology (CNPH) |

“The most effective way to do it,
is to do it.”
*-Amelia Earhart-*

**Sifra Blok**
Master Thesis
13-4-2021
Technical Medicine

University of Twente, Technical Medicine, Faculty of Science and Technology
University Medical Centre Utrecht, Department of Clinical Neurophysiology

UNIVERSITY OF TWENTE.

UMC Utrecht

# Index

List of abbreviations ..... 5
Abstract ..... 6
**Chapter 1 Background Information ..... 8**
Epilepsy ..... 9
SPES ..... 10
Intra-operative SPES ..... 12
Simulating SPES in an NMM ..... 12
**Chapter 2 Retrospective Analysis ..... 14**
Abstract ..... 15
Background ..... 15
Method ..... 16
Results ..... 17
Discussion ..... 22
**Chapter 3 Prospective Analysis ..... 25**
Abstract ..... 26
Background ..... 26
Method ..... 28
Results ..... 29
Discussion ..... 32
**Chapter 4 Analysis of a computational model ..... 34**
Abstract ..... 35
Background ..... 35
Method ..... 37
Results ..... 37
Discussion ..... 40
**Chapter 5 General discussion and general conclusion ..... 42**
**References: ..... 45**
**Appendix A: ..... 49**
**Appendix B: ..... 55**
**Appendix C: ..... 61**
**Appendix D: ..... 64**

# List of abbreviations

| Abbreviation | Description |
|---|---|
| BC | Betweenness centrality |
| CCEP | Cortico-Cortical Evoked Potential |
| DR | Delayed Response |
| ECoG | Electrocorticography |
| EEG | Electroencephalography |
| ER | Early Response |
| EZ | Epileptogenic Zone |
| GABA | Gamma (γ)-aminobutyric acid |
| HFO | High Frequency Oscillations |
| IEMU | Intensive Epilepsy Monitoring Unit |
| OR | Operating Room |
| NMM | Neural Mass Model |
| SOZ | Seizure Onset Zone |
| SPES | Single Pulse Electrical Stimulation |
| UMCU | University Medical Centre, Utrecht |

# Abstract

**Introduction:** Epilepsy is a major neurological disorder defined by a predisposition to recurrent unprovoked seizures. Epilepsy surgery is an optional treatment for patients with focal epilepsy. This is applied around 200 times per year in the Netherlands. In 20% of these patients, invasive EEG is required to delineate the epileptogenic zone (EZ) because this cannot be achieved using non-invasive methods alone. Subdural electrocorticography (ECoG) is one of those invasive EEG methods. After implantation of ECoG electrodes, Single Pulse Electrical Stimulation (SPES) can be performed on all electrodes. The physiological cortical responses to SPES are called cortico-cortical evoked potentials (CCEPs). CCEPs can be divided into Early Responses (ERs) and Delayed Responses (DRs). DRs help with delineating the EZ and have a peak of at least 100 ms after stimulation. ERs have consistent behaviour and show a sharp deflection (N1) between 9 and 100 ms after the stimulation pulse. An ER reflects an underlying cortico-cortical connection. A typical ER consists of an N1- and P1-peak. These are sometimes followed by a slow wave called the N2-peak. Mapping ERs is a method to reveal part of the brain's network. Currently, we perform SPES during an intensive seizure monitoring period awaiting spontaneous seizures. An alternative would be to perform SPES in the operating room (OR) while the patient is anaesthetised. The ECoG electrodes can be placed on the cortex after which SPES can be performed during surgery. Then the epileptogenic zone (EZ) can be found followed by surgical resection of the EZ. This would make the need to wait for seizures during the intensive monitoring week redundant. Propofol is the most popular anaesthetic for induction and maintenance of general anaesthesia. Propofol causes a prolongation of the actions of the slow and fast inhibitory populations. It is therefore hypothesised that the peak latencies of the N1-, P1- and N2-peaks will increase. ERs can be simulated with a Neural Mass Model (NMM). These simulations might explain the observed peak differences of ERs in agreement with the known inhibitory effect of propofol.

**Methods:** The medical ethical committee of the UMC Utrecht approved a protocol to perform SPES on anaesthetised patients, provided that the surgical procedure would not suffer a time delay. This meant that we had to reduce the duration of SPES. We first performed a retrospective analysis in six patients to determine whether a subset of two stimuli per stimulation pair instead of using the regular ten stimuli would suffice to determine the underlying cortico-cortical network. We compared the absolute number of ERs evoked per stimulation pair and we used network characteristics to determine the correlation between the networks. These were the total, positive and negative agreement, the in-degree, out-degree and betweenness centrality (BC). A sufficient correlation of these network characteristics implies that electrodes maintain the same function and importance within a network. This study was followed by a prospective analysis in which we included six patients who underwent ECoG recording in 2020 at the UMC Utrecht. We performed the regular SPES and an extra, shortened SPES in the OR. We calculated the same network characteristics as during the retrospective analysis. We determined the N1- and P1 latencies of the ERs in all six patients, and the N2-latencies in one patient. During the analysis of the computational model, we decreased the value of the gain and time constant of the fast inhibitory

populations in the NMM. We simulated ERs as a response to a regular SPES, and as a response to SPES performed in a propofol-anaesthetised patient.

**Results:** In the retrospective analysis, all patients showed a lower number of ERs evoked per stimulation pair for the setting in which we used 2 stimuli per stimulation pair. Between the 2 stimuli setting and the 10 stimuli setting, we found a high median overall and negative agreement of 93% and 96%, respectively. The positive agreement was lower with 71%. Five out of six patients showed a significant positive correlation ($p<0.05$) between the in-degree, out-degree and BC value. During the prospective analysis, all patients showed that fewer ERs were evoked per stimulation pair during the intra-operative SPES compared to regular SPES. We found a high median overall and negative agreement of 90% and 94%, respectively. The positive agreement was 53%. The network characteristics showed significant correlations ($p<0.05$) for at least four out of the six patients between the clinical-SPES and the propofol-SPES. During clinical-SPES, we found a median N1-, P1- and N2-latency of 23 ms, 59 ms and 208 ms, respectively. During propofol-SPES the N1-, P1- and N2-latencies increased to 28 ms, 68 ms and 220 ms, respectively. During the analysis of the computational model, we found that decreasing the time constant of the inhibitory populations led to increased peak latencies. We simulated an ER with latencies similar to the in vivo experiment by decreasing the gain of the fast inhibitory population from 25 $mV$ to 11 $mV$ and decreasing the time constant from 300 $s^{-1}$ to 175 $s^{-1}$.

**Conclusion:** From the retrospective analysis, we concluded that the network characteristics of SPES with two stimuli per stimulation pair showed a sufficient correlation with the regular SPES with ten stimuli. This implied that a similar cortico-cortical network can be captured with 2 stimuli. From the prospective analysis, we concluded that performing SPES in propofol-anaesthetised epilepsy patients is feasible and that, for four out of six patients, propofol did not interfere with the functional connectivity of electrodes in a network based on evoked ERs. More patients should be included to generate higher reliability of the conclusion. The analysis of the computational model showed that characteristics of ECoG responses with the influence of propofol changed as predicted. We concluded that an NMM with an adaptation of the inhibitory populations suffices to invoke the experimentally observed effect of propofol on an ECoG response.

# Chapter 1
# Background Information

## Epilepsy

Epilepsy is a neurological disorder defined by a predisposition to recurrent unprovoked seizures [1]. These seizures are caused by an imbalance between excitation and inhibition leading to excessive, hypersynchronous discharges of neurons in the brain [2]–[4]. In 2019 in the Netherlands, epilepsy was diagnosed 11.000 times, the prevalence of epilepsy was 60.500. In the coming 25 years, it is expected that this number will continue to increase by 10%, this is mainly due to ageing [5]. In 2019, 291 individuals died because of epilepsy. This number has more than doubled in 40 years.

According to the Dutch national guidelines, epilepsy surgery should be explored in all patients with persistent seizures after two consecutive years of medical treatment or when three first-line antiepileptic drugs have failed. Epilepsy surgery is performed 200 times per year in the Netherlands [6]. Surgery is a highly effective treatment in patients with focal neocortical epilepsy, leading to seizure-freedom in 50-75% of patients [7]–[12]. Traditionally, epilepsy surgery depends on finding the epileptogenic zone (EZ) and delineating it from the eloquent cortex, such as the motor, visual or language areas. The EZ is the area of the cortex that is indispensable for the generation of epileptic seizures and the removal of which is necessary for the complete abolition of seizures [13], [14]. The EZ is often approximated with the seizure onset zone (SOZ) which is the area of the cortex that generates seizures with clinical symptoms [15]. Recently, the field of interest in epilepsy surgery shifted towards studying the importance of network disconnection instead of the removal of a localised EZ [16]–[18].

In 20% of the patients, invasive EEG is required to delineate the EZ because this cannot be achieved using non-invasive methods alone [19]–[22]. Subdural electrocorticography (ECoG) is one of the invasive EEG methods. The current capacity of ECoG measurements is approximately 10 patients per year at the University Medical Centre, Utrecht (UMCU). For ECoG, a craniotomy is performed to place a multi-electrode grid directly on the cortex, see *Figure 1.1*. After implantation of ECoG electrodes, patients stay in the hospital for approximately seven days and have to stay in bed for the entire period. Patients can be monitored continuously awaiting an epileptic seizure to delineate the SOZ [23]. Seizure monitoring has to cope with the inherent unpredictability of seizures. Seizures are often precipitated by withdrawal of medication. This poses the patient at the risk of developing more severe seizures than usual, sometimes leading to status epilepticus that requires acute intervention. It is therefore important to study possibilities in finding the EZ that would make this invasive monitoring period redundant.

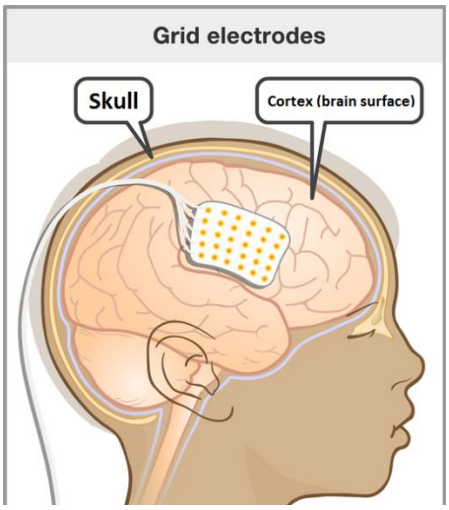


*Figure 1.1: Example of grid electrodes placed on the cortex to perform ECoG measurements. Each yellow dot represents an electrode. This figure is adapted from a figure in* [24].

## SPES

Single Pulse Electrical Stimulations (SPES) can be performed on epilepsy patients with chronically implanted ECoG electrodes. Previous research [2], [3], [25]–[27] has shown that SPES is a valuable test to reveal the SOZ without relying on spontaneous events such as seizures or interictal discharges. SPES can also be used to track functional connectivity among different cortices and explain seizure propagation [16], [26], [28], [29]. Epileptic seizures are caused by an imbalance between excitation and inhibition of cortical areas [4]. It is thought that with single pulses such an imbalance is triggered and epileptogenic tissue can be identified [2], [3].

During SPES, ten short electrical pulses of 1 ms are applied between two adjacent electrodes (stimulation pair). Each stimulation pair is stimulated 10 times with a 5-second stimulus-interval to allow electrodes to depolarise after each pulse and for the brain to recover to baseline status [2]. Each stimulation pair is stimulated 5 times in each direction/polarity, see *Figure 1.2A.* Stimulating in both directions minimises the influence of the stimulation artefact when averaging all stimuli, see *Figure 1.2B.* Pulses have a current intensity of 8 $mA$. Electrodes on the pre- and post-central gyrus are often stimulated with 4 $mA$ to decrease the risk of evoking muscular activity in the extremities or facial area. On average, performing SPES lasts approximately 60 minutes.

The chance that SPES provokes a seizure is extremely low, and the reproducibility of the data is very high [2], [28]–[32]. Only a limited and localised population of neurons is activated because of the short duration of the pulses and the long inter-stimulus interval. It is more likely to produce massive and widespread cortical activation when 1) the duration of the pulses is longer, 2) the amplitude of the pulses increases or when 3) the pulses are applied with smaller inter-stimulus interval, [2], [3].

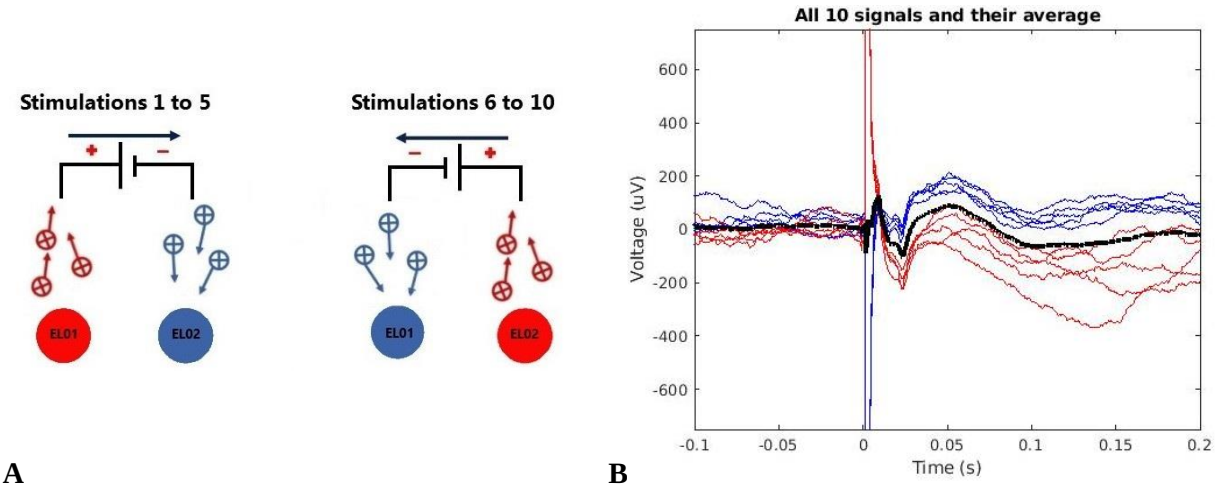


**A** **B**

*Figure 1.2: A) During SPES, each stimulation pair (EL01-EL02) is stimulated 10 times, 5 times in each direction/polarity. B) Averaging the 10 stimuli in positive (red) and negative (blue) direction results in a reduction of the stimulation artefact (black).*

**Cortical responses to SPES**

The physiological cortical responses to SPES are called cortico-cortical evoked potentials (CCEPs). CCEPs can be divided into Early Responses (ERs) and Delayed Responses (DRs). DRs can be observed in electrodes placed on epileptic tissue after stimulation elsewhere and can help with delineating the EZ [2], [3], [25], [26], [29]. DRs consist of one or several typical spike-and-slow waves, resembling interictal epileptiform discharges with a delay longer than 100 ms after stimulation [33]. DRs occur stochastically, and this is one of the reasons that each stimulation pair is stimulated 10 times. Note that for this thesis, SPES responses based on two stimuli per stimulation pair were considered, making DR analysis not feasible. ERs have consistent behaviour and show a sharp deflection (N1) between 9 and 100 ms after the stimulation pulse. ERs provide insight into eloquent brain networks such as language, cognitive and motor networks and can be used explain seizure propagation [2], [25], [26], [29], [30], [34], [35]. A typical ER, as shown in *Figure 1.3*, consists of an N1- and P1-peak. These are sometimes followed by a slow wave called the N2-peak [34], [36]. The amplitude of ERs depends on the stimulation intensity, often the maximum amplitudes are found at electrodes close to the stimulation pair electrodes [2], [27], [36], [37].

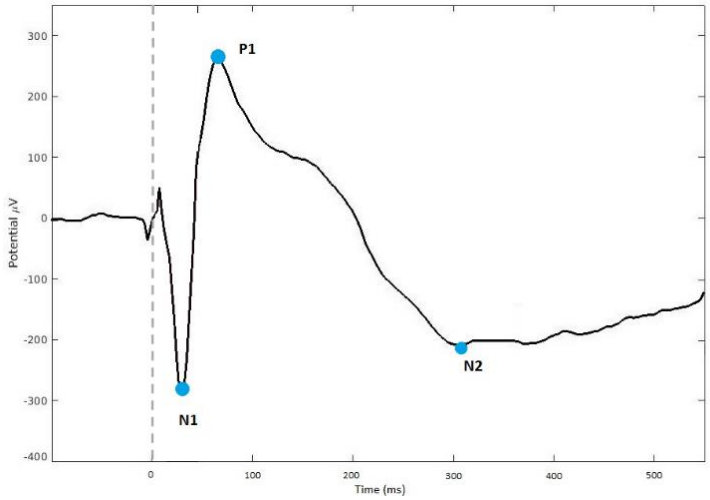


*Figure 1.3: Example of characteristic ER, first a sharp negative deflection occurs (N1) followed by a positive peak (P1). This is sometimes followed by a slow wave (N2). The stimulation is generated at Time = 0 ms.*

## Intra-operative SPES

In some patients, the expected EZ is not on the eloquent cortex. In these patients, performing SPES might be sufficient to determine the location that needs to be removed for the complete abolition of seizures. This could be the EZ or tissue that is an important controller of the propagation of a seizure. When this is the case, SPES could be performed directly in the OR after the electrode placement. The EZ can be found followed by resection of the EZ all during the same procedure. This would make the need to wait for seizures during the intensive monitoring week redundant.

The most popular anaesthetic for induction and maintenance of general anaesthesia is propofol. The effect of propofol is the potentiation of the inhibitory neurotransmitter γ-aminobutyric acid (GABA) at the $GABA_A$-receptor [38], [39]. Propofol enhances the inflow of chloride that hyperpolarises the postsynaptic membrane and therefore inhibits neuronal depolarisation [38]–[40]. This leads to an inhibition of neurotransmission.

We do not yet fully know the effect of propofol on ERs evoked during SPES. Propofol has an anti-epileptic effect and propofol produces a dose-dependent depression of the EEG [19], [21], [39], [41]. *Yamao et al. (2014)* performed SPES in propofol-anaesthetised patients [28]. They studied intra-operative language mapping methods and compared ERs evoked under general anaesthesia with ERs evoked while the patient was awake during awake craniotomy. They reported that the CCEP distribution did not change (i.e., did not get wider) and they reported no decisive change of the duration between the stimulation pulse and the N1-peak.

## Simulating SPES in an NMM

The field of mathematical modelling of epilepsy has grown rapidly over the past decades [35], [42]–[45]. Neural Mass Models (NMMs) can be used to, ex vivo, describe the average neuronal activity of a

population. NMM use a small number of variables, this enables studying the essential features necessary for a particular dynamic behaviour [46], [47]. An often-used model is the Wendling model [48]. The model simulates a single neural mass containing four neuronal populations, i.e., the pyramidal, excitatory, slow inhibitory and fast inhibitory population. Each population has a mean membrane potential (MMP) that is influenced by other populations or external inputs via synaptic transmissions. Pyramidal cells are considered as the main population in the NMM [35], [48], [49]. The MMP of the pyramidal population is obtained by multiplying the output of each population by the connectivity constant and then adding up the MMP of the excitatory population and subtracting the MMP of the inhibitory populations.

*Hebbink et al. (2020)* [37] adapted the Wendling model by adding feedforward inhibition, see *Figure 1.4*. Feedforward inhibition generates the long-range effect of epileptic activity and is, therefore, a critical determinant to simulate the seizure dynamics in the EEG [50]. They used that model to study ECoG responses to SPES which they modelled using a short, transient external input (block pulse). Every single neural mass represents the tissue underneath an electrode of the ECoG grid. Considering the action of propofol, it is hypothesised that, an ECoG response to SPES in a propofol-anesthetised patient can be simulated by changing the parameter setting of the inhibitory populations.

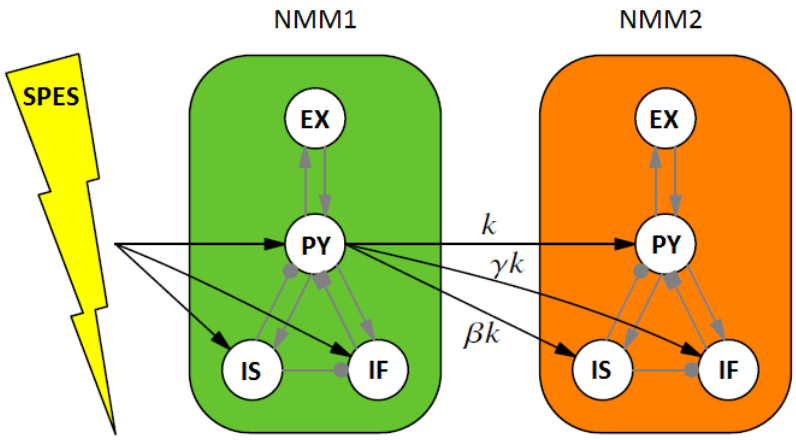


*Figure 1.4: Feedforward coupled neural masses as proposed by Hebbink et al. (2020)* [37]. *Feedforward inhibition between NMM1 and NMM2 (factor k) is added to this model in order to simulate the long-range effect of epileptic activity. This figure is adapted from a figure in* [37].

# Chapter 2
# Retrospective Analysis

## Abstract

**Objective** In this chapter, we investigate whether a subset of 2 stimuli per stimulation pair could be used to obtain a network with the same functional connectivity as a network based on 10 stimuli per stimulation pair. In the next chapter, a prospective study is described in which we apply SPES in the OR. To save time in the OR, it is important to confirm that a cortico-cortical network can be derived from two stimuli.

**Method** We included six epilepsy patients in whom SPES had been performed during chronic clinical ECoG monitoring. We averaged the responses to 10 stimuli per stimulation pair and we averaged a subset of the responses to 2 stimuli per stimulation pair. We used an automatic detector to detect Early Responses (ERs) in the averaged signal of both settings. We compared the number of ERs evoked per stimulation pair, we calculated the agreement, and we determined the correlation of the in-degree, out-degree, betweenness centrality and the number of ERs evoked per stimulation pair.

**Results** All patients showed a lower absolute number of ERs evoked per stimulation pair for the 2 stimuli setting. We found a high median overall and negative agreement between the 10 stimuli setting and the 2 stimuli setting of 93% and 96%, respectively. The positive agreement was slightly lower with 71%. The network characteristics showed a significant correlation ($p<0.05$) for at least five out of the six patients between the 2 stimuli and the 10 stimuli setting.

**Conclusion** We concluded that the network characteristics of SPES with 2 stimuli per stimulation pair showed a sufficient correlation with the network characteristics of SPES with 10 stimuli per stimulation pair. An equal cortico-cortical network can be captured with 2 stimuli.


## Background

In this chapter, we investigate whether a subset of 2 stimuli per stimulation pair could be used to obtain a network with the same functional connectivity as a network based on 10 stimuli per stimulation pair. In the next chapter, we will perform SPES in the OR for which limited time is available. A complete SPES protocol as performed during chronic ECoG monitoring lasts on average 60 minutes, so we need to shorten this protocol. To obtain a shorter stimulation protocol, we wanted to adjust the regular SPES protocol by stimulating all stimulation pairs 2 times instead of 10 times. Traditionally, Delayed Responses (DR) have been used to delineate the epileptogenic zone (EZ), since DRs have a stochastic behaviour, it is necessary to stimulate each stimulation pair 10 times. Early Responses (ERs) however, occur consistently and it is therefore believed that two stimuli per stimulation pair will be sufficient to detect and study ERs [36].

There are several topological characteristics to describe a network based on ERs, for example, the in-degree, out-degree and the betweenness centrality (BC) [23], [51], [52]. The in-degree is a measure for the number of edges directed towards a specific electrode (i.e. number of ERs evoked in a specific electrode). The out-degree is a measure of edges directed away from a certain electrode (i.e. the number of ERs evoked after stimulating that electrode). Both the in- and out-degree reflect the importance of an

electrode in the network. The BC is defined as the fraction of all shortest paths in the network that pass through a given node [52]. Electrodes with a high BC are often important bridges that connect parts of the network.

It was hypothesised that, based on the consistent occurrence of ERs, the 2 stimuli setting and the 10 stimuli setting would result in significantly correlating outcomes of the network characteristics.

# Method

### Patient characteristics

We included patients from the RESPect database who underwent grid recordings in 2018 at the UMC Utrecht [53]. Since 2018, stimulation pairs were stimulated in both directions. SPES was performed as part of clinical procedures which was explained in more detail in *Chapter 1.2*. The sample size of the study population was matched to the number of patients we expected to include in the prospective analysis of this thesis (see *Chapter 3*). No other inclusion or exclusion criteria were used.

### Analytical settings

We compared two settings. The first setting contained 10 stimuli per stimulation pair. It contains 5 stimuli in the positive and 5 stimuli in the negative direction that were averaged to one signal, see *Figure 2.1A&B*. The second setting contained a subset of 2 stimuli per stimulation pair. We averaged the first stimulus in the positive direction and the first stimulus in the negative direction, see *Figure 2.1C&D*. Hence, the 2 stimuli setting used a subset of the data that was used in the 10 stimuli setting. We used the automatic detector validated by *van Blooijs (2015)* to detect the ERs in each averaged response [54].

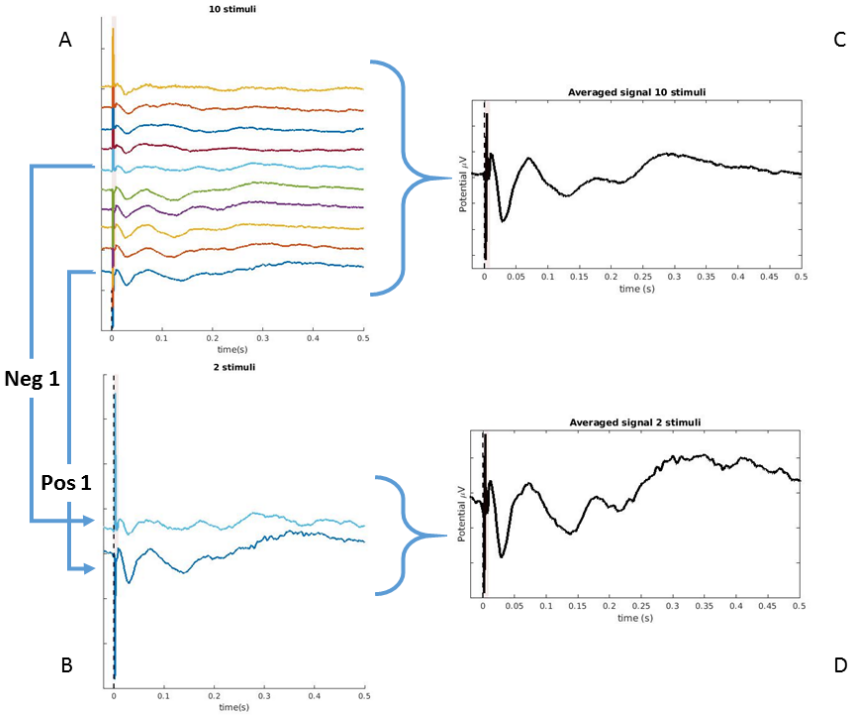


*Figure 2.1: A) All responses in one electrode after 10 stimuli to a stimulation pair. B) The responses of the first stimulus in the positive direction and the first stimulus in the negative direction of the same electrode as in A. C&D) The averaged signals of the signals in A and B, respectively.*

**Overall, positive and negative agreement**

The overall, positive and negative agreement were calculated using *Equations 2.1 – 2.3* and the matrix shown in *Table 2.1*. A median and Inter Quartile Range (IQR) was determined for all patients.

*Table 2.1: Matrix used to determine the agreement between the 2 stimuli setting and the 10 stimuli setting.*

| | | **10 stimuli setting** | |
|---|---|---|---|
| | | **Detected ER** | **No detected ER** |
| **2 stimuli setting** | **Detected ER** | True Positive (TP) | False Negative (FN) |
| | **No detected ER** | False Positive (FP) | True Negative (TN) |

$$agreement_{overall} = \frac{TP + FN}{TP + TN + FP + FN} * 100\% \quad [2.1]$$

$$agreement_{positive} = \frac{2 * TP}{2 * TP + FP + FN} * 100\% \quad [2.2]$$

$$agreement_{negative} = \frac{2 * TN}{FP + FN + 2 * TN} * 100\% \quad [2.3]$$

**Network characteristics**

We compared the absolute number of ERs evoked per stimulation pair for the 2 and 10 stimuli setting. We also calculated the correlation between the two settings for the following network characteristics; the number of ERs evoked per stimulation pair, the in-degree per electrode, the out-degree per electrode and the BC per electrode [51], [52]. The in-degree, out-degree and BC were normalised by considering the number of stimulation pairs an electrode was part of, calculations are described in detail in *van Blooijs et al. (2018)* [23]. These network characteristics were chosen because they ignore connection weights in their calculations and could be calculated based on whether an ER was present or absent.

**Statistical analysis**

We used the non-parametric *Wilcoxon Signed Rank test* to compare the absolute number of ERs detected per stimulation pair for all patients.

We used a *Spearman correlation* to determine the correlation between the network characteristics of the two settings. The strength of the correlation was expressed with the correlation coefficient ($r_s$).

# Results

**Patient Characteristics**

We selected 6 patients (5 female) from the RESPect database [53]. They had a median age of 27 years (range: 9-50) who all underwent grid implantation and clinical SPES as part of the clinical routine at the Department of Clinical Neurophysiology at University Medical Centre, Utrecht, see *Table 2.2*.

*Table 2.2: Characteristics of patients included in the retrospective analysis.*

| Patient number | Age at grid implantation | Gender | Hemisphere |
|---|---|---|---|
| RESP0701 | 30 | F | Right Temporal, |
| RESP0702 | 30 | F | Left Temporo-parietal |
| RESP0703 | 15 | F | Left Temporo-parietal |
| RESP0706 | 50 | F | Right Frontal |
| RESP0724 | 9 | M | Right Temporo-parieto-occipital |
| RESP0728 | 9 | F | Left Frontal |

**Overall, positive and negative agreement**

The median overall agreement of all patients was 93% (IQR 91 - 94%). The median positive agreement of all patients was 71% (IQR 44 - 72%). The median negative agreement of all patients was 96% (IQR 95 - 96%). The agreements per patient are shown in *Table 2.3*.

*Table 2.3: Overall, positive and negative agreement between the ERs detected in the average signals of 2 stimuli and 10 stimuli per patient.*

| Patient number | Overall (%) | Positive (%) | Negative (%) |
|---|---|---|---|
| RESP0701 | 91 | 72 | 95 |
| RESP0702 | 94 | 74 | 96 |
| RESP0703 | 93 | 71 | 96 |
| RESP0706 | 94 | 71 | 97 |
| RESP0724 | 92 | 44 | 96 |
| RESP0728 | 88 | 30 | 93 |

**Comparison of the absolute number of ERs evoked per stimulation pair**

In all patients, a higher or the same number of ERs was detected in the 10 stimuli setting compared to the 2 stimuli setting, see *Figure 2.2.* RESP0724 and RESP0728 showed a significant decrease for the results of the 2 stimuli setting ($p < 0.001$). During the 2 stimuli setting, on average for all patients, 2.5 times fewer ERs were detected compared to the 10 stimuli setting (range 1- 6 times fewer ERs).

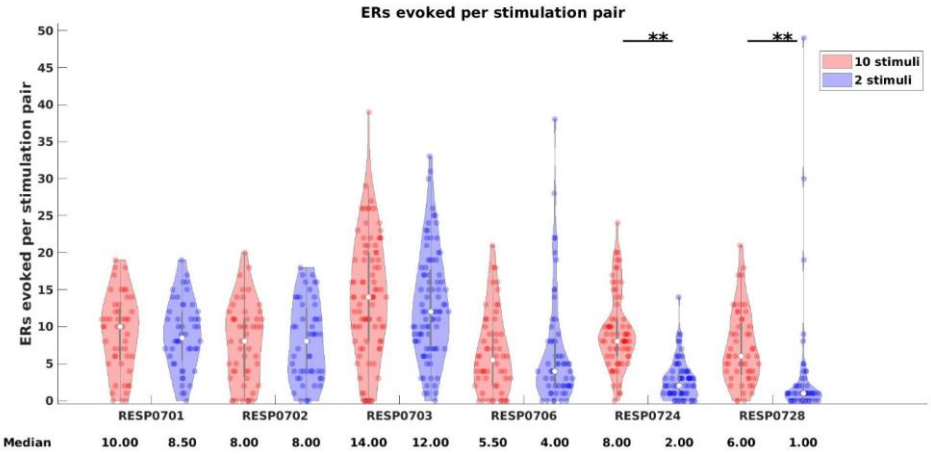


*Figure 2.2: Number of ERs evoked per stimulation pair, in red the 10 stimuli setting and in blue the 2 stimuli setting. Each marker represents a stimulation pair. (** = p <0.001).*

**Correlation of the ERs per stimulation pair**

All patients showed a positive correlation (at least, $p<0.05$) between the number of ERs evoked per stimulation pair of the 2 and 10 stimuli setting, see *Figure 2.3*. On average, 1.3 times more ERs were detected per stimulation pair during the 10 stimuli setting (IQR 1.2 – 4 times).

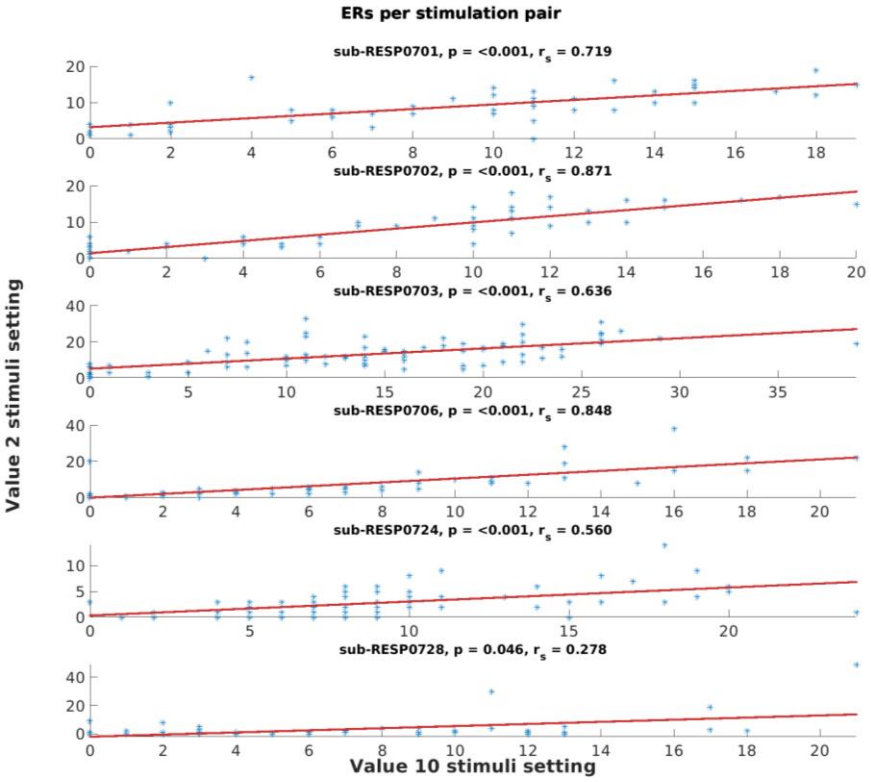


*Figure 2.3: Scatter plot of the ERs evoked per stimulation pair for all patients. Each marker represents a stimulation pair with on the x-axis the number of ERs for the 10 stimuli setting, and on the y-axis the number of ERs for the 2 stimuli setting. The $r_s$ indicates the strength of the correlation.*

RESP0728 showed the weakest correlation ($r_s = 0.278$) and RESP0702 showed the strongest correlation ($r_s = 0.871$). In *Figure 2.4* we visualised the ranking of the stimulation pairs based on the number of ERs they evoked during the 2 stimuli and the 10 stimuli setting. The figure shows that subjects with a high correlation (RESP0702) showed more horizontal lines.

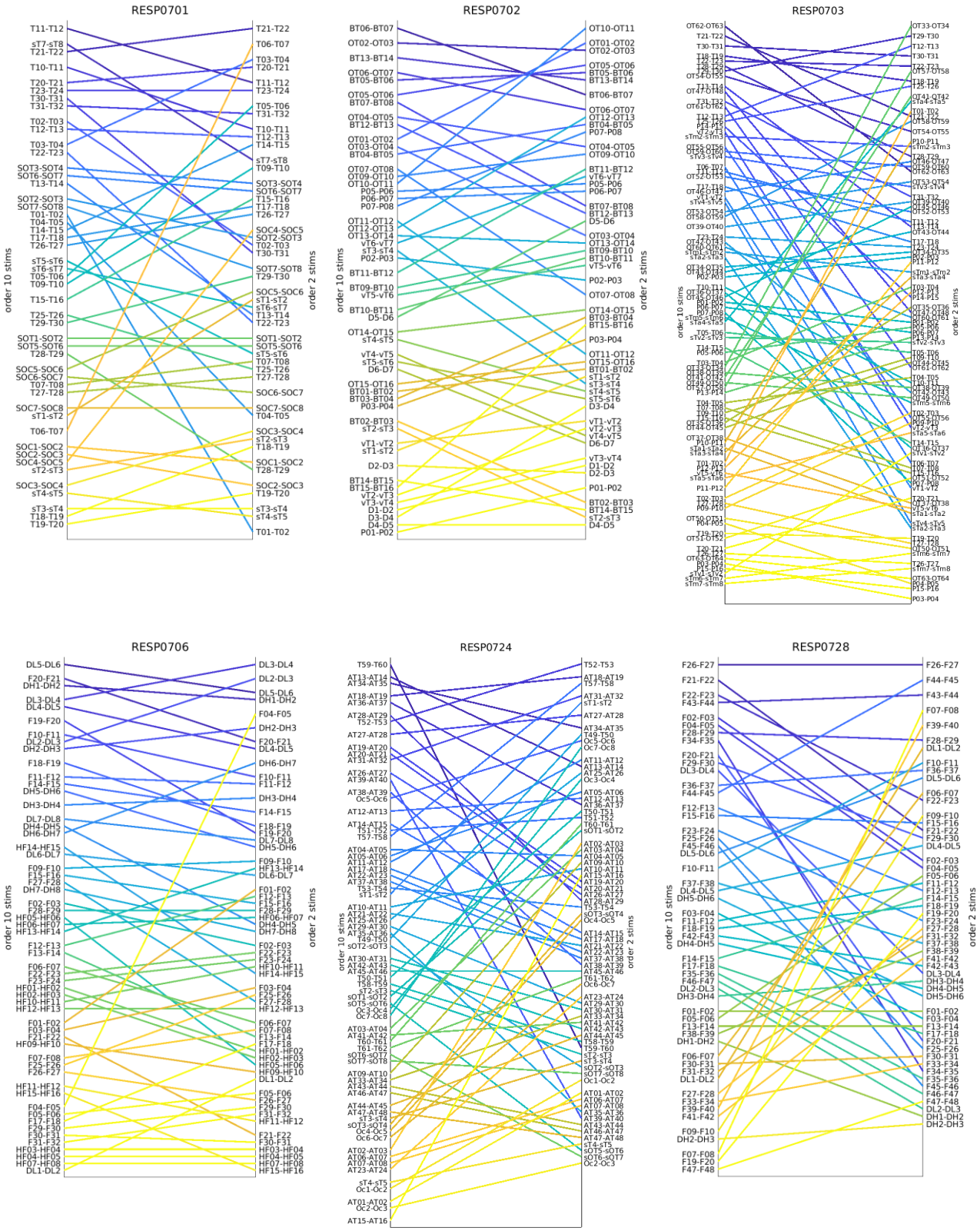


*Figure 2.4: The stimulation pairs were ranked based on the number of ERs they evoked. On the left vertical axis of each sub-figure, the ranking of the 10 stimuli setting is shown. The ranking of the 2 stimuli setting is indicated on the right axis. A line is drawn between the same stimulation pair in both rankings. More horizontal lines indicate that stimulation pairs remained the same place in the ranking. Stimulation pairs with the same number of ERs are grouped.*

**Correlation of the in-degree, out-degree and betweenness centrality**

All patients showed a positive correlation (at least, $p<0.05$) between the in-degree of the 2 stimuli and the 10 stimuli settings, see *Figure 2.5*. All patients, except RESP0728, showed a positive correlation (at least, $p<0.05$) for the out-degree and the BC.

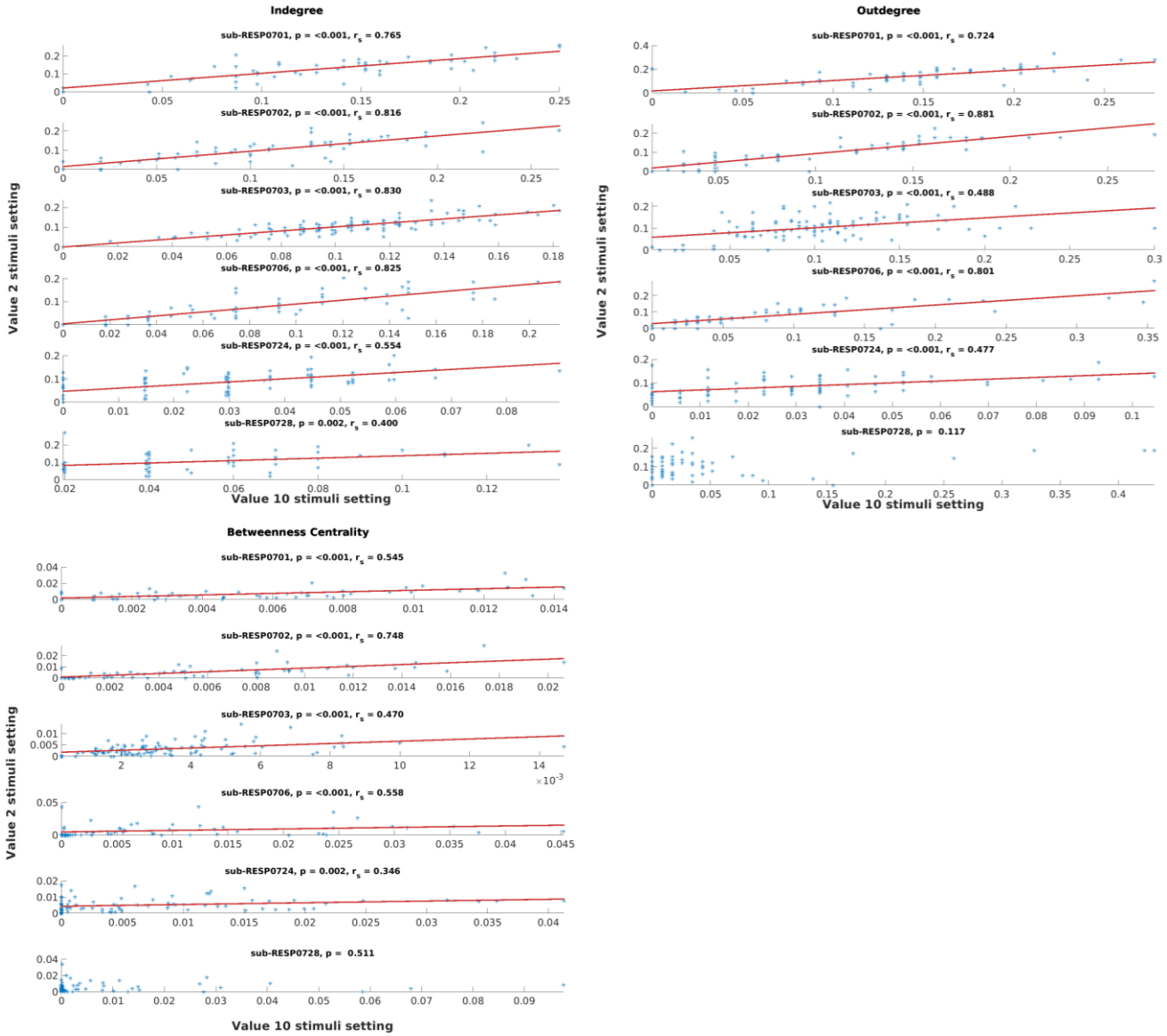


*Figure 2.5: Scatter plots of the normalised in-degree, out-degree and betweenness centrality of all six patients. Each marker represents an electrode with on the x-axis the value for the 10 stimuli setting, and on the y-axis the value for the 2 stimuli setting. The $r_s$ indicates the strength of the correlation.*

Network characteristics with a strong correlation ($r_s > 0.7$) contained electrodes that maintained the same place when ranked from high to low, see *Figure 2.6.* The 2D grid visualisation for the network characteristics of all patients is provided in *Appendix A.*

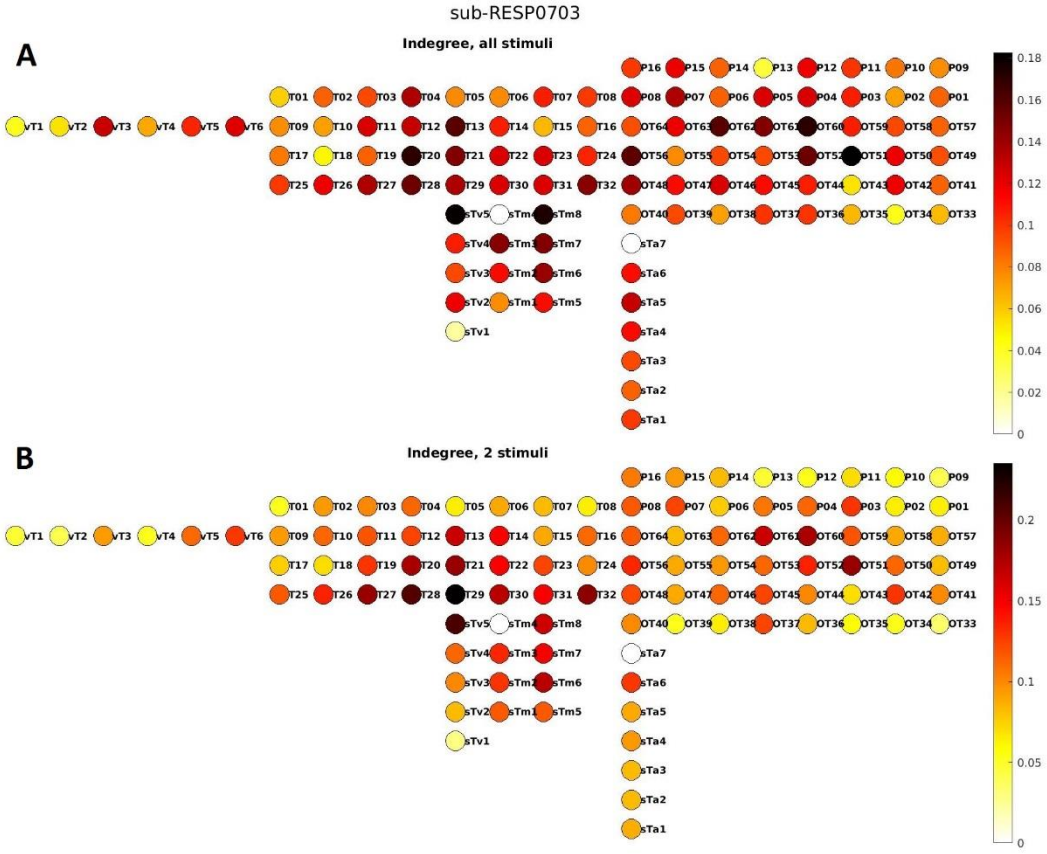


*Figure 2.6: The 2D grid visualisation of the in-degree values for RESP0703 for the A) 10 stimuli setting and B) 2 stimuli setting. Different scales for the colour bar were used to show that the electrodes with the highest in-degree in the setting with 10 stimuli still had the highest in-degree in the 2 stimuli setting.*

# Discussion

In this chapter, we studied whether a subset of 2 stimuli per stimulation pair could be used to obtain a network with the same functional connectivity as a network based on 10 stimuli per stimulation pair. It was hypothesised that both settings would result in correlating outcomes of the network characteristics based on ER analysis.

The overall and negative agreement between the 2 stimuli setting and the 10 stimuli setting was high for all patients, all above 80%. While none of the patients showed a high positive agreement. This was probably caused by the high number of signals without an ER, compared to the number of signals that did show an ER. This makes that a false negative detection had a great effect on the positive agreement. We found a significantly lower number of ERs per stimulation pair when 2 stimuli were used ($p<0.001$) for RESP0724 and RESP0728. All patients showed a significant correlation with the number of evoked ERs per stimulation pair. This indicates that stimulation pairs were ranked similarly for the 2 and 10 stimuli setting, which suggests that the importance of an electrode in a network was similar in both

settings. The in-degree, out-degree and BC showed significant correlations between the 2 stimuli setting and the 10 stimuli setting for all patients, except for RESP0728.

**Patient RESP0728**

Patient RESP0728 showed a particularly low positive agreement and was the only patient without a significant correlation for the out-degree and the BC. It was found that the two signals used for the 2 stimuli setting, often showed a large difference in amplitude (µV), see *Figure 2.7 (left)*. This resulted in an incoherent averaged signal which led to an incorrect ER detection. This effect was not found when averaging the second positive stimulus and the second negative stimulus, see *Figure 2.7 (right)*. The overall agreement increased from 87% to 96%, the positive agreement doubled from 34% to 67%, and the negative agreement increased from 93% to 98%. It was later found that incorrect equipment set-up led to this phenomenon. A visual check of the responses could have avoided this misdetection. Another solution would have been to re-reference by using a common average reference.

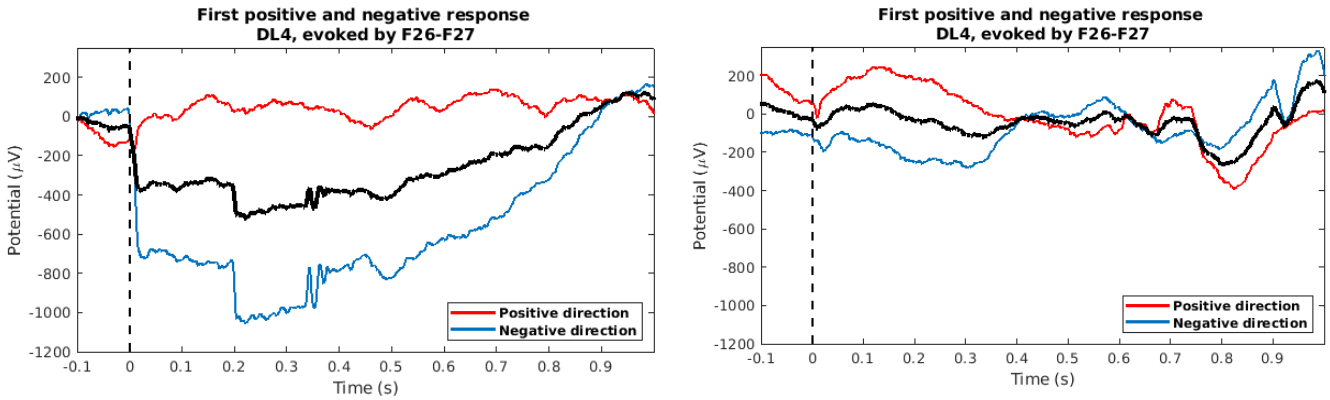


*Figure 2.7: Left: the responses to the first positive (red) and first negative (blue) stimulus and their averaged signal (black) used for the 2 stimuli setting of RESP0728. An ER is detected in this response by the automatic detector. Right: the responses to the second positive (red) and negative (blue) stimulus of the same electrode-stimulation pair combination.*

A limitation of this study was that we did not perform a visual check of the automatically detected ERs while we knew that the detector was not validated for ER detection in a signal based on 2 stimuli. The detector only considers the averaged signal when selecting an ER. An observer could also check whether each separate response results in an ER, see *Figure 2.8*. The visual check was not performed because it is a time-consuming task and because previous research concluded that the performance of the ER detector is sufficient for use in further research [54]. For future research, we would highly recommend performing a visual check to decrease false detection of ERs.

**A**

**B**

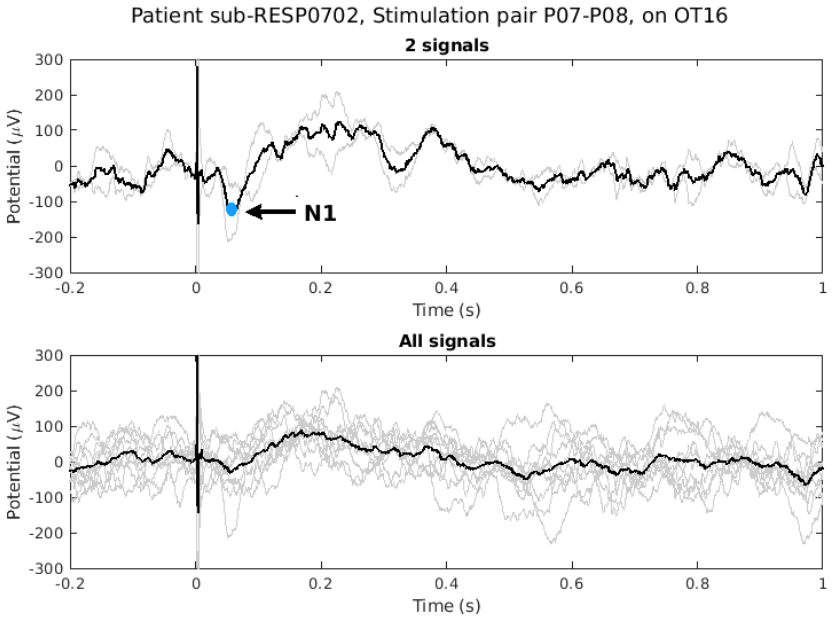


*Figure 2.8: Example of how averaging 2 signals can result in different ER detection compared to averaging 10 signals. A) The 2 stimuli (grey lines) with inconsistent responses and their average (black line) with an incorrectly detected N1 peak, see the blue marker. B) All signals (grey lines) and their average signal (black). In this signal, no ER was detected.*

We conclude that the network characteristics of SPES with 2 stimuli per stimulation pair showed a sufficient correlation with the network characteristics of SPES with 10 stimuli per stimulation pair. This implies that we could use a subset of 2 stimuli per stimulation pair to obtain a network with the same functional connectivity as compared to 10 stimuli per stimulation.

# Chapter 3
# Prospective Analysis [1]

[1] The introduction of Chapter 3 is a compact version of the background information of Chapter 1.

# Intra-operative SPES; the influence of propofol on local brain networks in epilepsy patients [2]

Sifra Blok,
Technical Medicine, University of Twente
Department of Clinical Neurophysiology, UMC Utrecht

April 13, 2021

## Abstract

**Objective**: Single Pulse Electrical Stimulation (SPES) can be used to reconstruct the underlying cortical network. A physiological cortical response to SPES is an Early Response (ER). A typical ER consists of an N1- and P1-peak. These are sometimes followed by a slow wave called the N2-peak. Currently, SPES is performed during a chronic intracranial grid monitoring period for clinical purposes. In this study, we investigated whether SPES performed in a propofol-anaesthetised patient showed the same cortical network compared to SPES performed during the intracranial grid monitoring period.

**Methods**: We included six epilepsy patients in whom we performed an extra SPES session in the operating room while they were anaesthetised with propofol. We used an automatic detector to detect ERs. The detected events were visually checked. We compared the number of ERs evoked per stimulation pair, we calculated the agreement, and we determined the correlation of the number of ERs evoked per stimulation pair, the in-degree, out-degree and for the betweenness centrality. For each patient, we determined the median N1- and P1-latency during the regular SPES and during the intra-operative SPES. We determined the median N2-latencies in one patient.

**Results**: For all patients, we found that fewer ERs were evoked per stimulation pair during the intra-operative SPES compared to regular SPES. We found a high median overall and negative agreement of 90% and 94%, respectively. The positive agreement was 53%. The network characteristics showed a significant correlation ($p<0.05$) for at least four out of the six patients between the clinical-SPES and the propofol-SPES. We found an increase of the N1-, P1- and N2-latencies during propofol-SPES. The N1-, increased from 23 ms to 28 ms, the P1-latency increased from 59 ms to 68 ms and the N2-latency increased from 208 ms to 220 ms.

**Conclusions**: We concluded that performing SPES in propofol-anaesthetised epilepsy patients is feasible and that propofol does not interfere with the functional connectivity of electrodes in a network based on evoked ERs.

**Keywords**

Electrocorticography, epilepsy, network characteristics, propofol, single-pulse electrical stimulation

## Background

Epilepsy surgery is a highly effective treatment in patients with focal neocortical epilepsy, leading to seizure-freedom in 50-75% of the patients [7]–[10]. Epilepsy surgery depends on finding the epileptogenic zone (EZ) and delineating it from the eloquent cortex,

[2] This chapter is written in a structure for an article using the guide for authors of Clinical Neurophysiology (Elsevier)

such as the motor, visual or language areas. The EZ is the area of the cortex that is indispensable for the generation of epileptic seizures and the removal of which is necessary for the complete abolition of seizures [13], [14]. In 20% of the patients, invasive EEG is required to delineate the EZ because this cannot be achieved using non-invasive methods alone [19]–[22]. Subdural electrocorticography (ECoG) is one of those invasive EEG methods. After implantation of ECoG electrodes, patients can be monitored continuously awaiting an epileptic seizure to delineate the Seizure Onset Zone (SOZ) [23]. The SOZ is an approximation of the EZ [15]. Seizure monitoring has to cope with the inherent unpredictability of seizures [55]. Seizures are often precipitated by withdrawal of medication. This poses the patient at the risk of developing more severe seizures, sometimes leading to status epilepticus that requires acute intervention. It is therefore important to study possibilities to make this invasive monitoring period redundant.

Single Pulse Electrical Stimulation (SPES) can be performed on patients with implanted ECoG-electrodes. Previous research [2], [3], [25]–[27] has shown that SPES is a valuable test to reveal the EZ without relying on spontaneous events such as seizures or interictal discharges. The physiological cortical responses to SPES are called cortico-cortical evoked potentials (CCEPs). When a sharp negative deflecting response (N1) occurs between 9 and 100 ms after the stimulation pulse, it is considered an Early Response (ER). ERs provide insight into eloquent brain networks such as language, cognitive and motor networks and can be used explain seizure propagation [2], [25], [26], [29], [30], [34], [35]. ERs occur consistently [36]. A typical ER consists of an N1- and P1-peak and these are sometimes followed by a slow wave called the N2, see *Figure 1*.

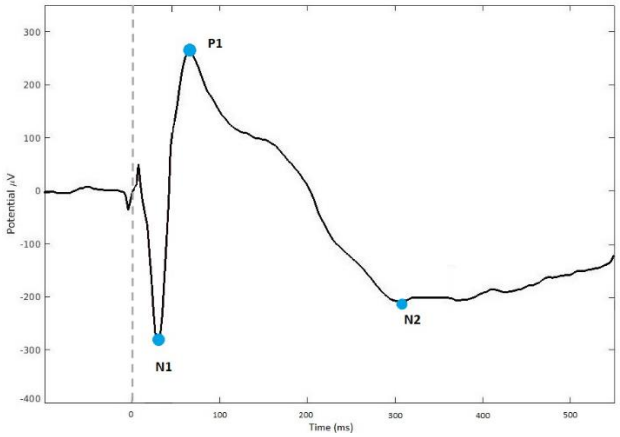


***Figure 1**: Example of a typical ER with at $t = 0$ ms the stimulation. The first negative peak is called the N1, the first positive is called P1 and these are sometimes followed by a second negative peak N2* [34]–[36].

Topological network characteristics like the in-degree, out-degree and betweenness centrality (BC) can be calculated to describe the network based on the evoked ERs [23], [51], [52]. The in-degree is a measure for the number of edges directed towards a specific electrode (i.e. number of ERs evoked in a specific electrode). The out-degree is a measure of edges directed away from a certain electrode (i.e. the number of ERs evoked after stimulating that electrode). The betweenness centrality (BC) is the fraction of all shortest paths in the network that pass through a given node [52]. Electrodes with a high BC are often important controllers of a network because it connects multiple areas of the brain.

In some patients, the expected EZ is not in the eloquent cortex. For those patients, merely performing SPES might be sufficient to delineate the EZ. A possible method is to perform SPES in the operating room (OR) while a patient is propofol-anesthetised (propofol-SPES). This could lead to the delineation of the EZ and functional areas during surgery and is therefore without the need to wait for seizures during an intensive monitoring period. We do not yet fully know the effect of propofol on ERs evoked during SPES. Propofol acts

on the $\gamma$-aminobutyric acid receptor ($GABA_A$-receptor), thereby causing an inhibitory effect on the neurotransmission [38]–[40]. It is also known that propofol has an anti-epileptic effect and that propofol produces a dose-dependent depression of the EEG [19], [21], [39], [41]. *Yamao et al. (2014)* performed SPES while the patient was under general anaesthesia and once while the patient was awake during awake craniotomy [28]. They reported that the CCEP distribution did not change (i.e., did not get wider) and they reported no decisive change of the duration between the stimulation pulse and the N1-peak. They did not compare their results to a network generated by SPES without any anaesthesia.

In this study, we investigated whether SPES performed in propofol-anaesthetised patients showed the same number of ERs and similar values for the in-degree, out-degree and BC compared to regular SPES as part of the clinical procedure. We hypothesised that the values found for these network characteristics during propofol-SPES would resemble the values of the regular SPES. The inhibitory effect of propofol will possibly lead to a lower absolute number of ERs and increased duration between the stimulation pulse and the N1-, P1- and N2-peaks.

# Method

Patients who received ECoG recordings in 2020 were asked to participate in the PRIOS-study *(Propofol IntraOperative SPES)*. All patients were fully informed of the nature of the research and gave informed consent. The experimental procedure complied with the Dutch law on Medical Research in Humans declared by the ethical committee of the University Medical Centre of Utrecht (non-WMO, reference number 20221/C).

**Stimulation protocols**

SPES was performed as part of the chronic clinical ECoG monitoring (clinical-SPES). This was performed under conditions of relaxed awareness when the patient had recovered from the implantation operation. This was usually 48 h after. During clinical-SPES, ten short electrical pulses of 1 ms were applied between two adjacent electrodes (stimulation pair). Pulses had a current intensity of 4-8 mA. Each stimulation pair was stimulated ten times and after five stimuli, the two electrodes switched their functions as cathode and anode. The ECoG signal was divided into epochs of two seconds before and three seconds after the stimulation artefact. The epochs of the ten stimuli were averaged to minimise the influence of the stimulation artefact and to increase the signal-to-noise ratio. We did not stimulate electrodes placed on top of other electrodes because of unknown current transfer. Due to limited time to perform the SPES in the OR, we stimulated each stimulation pair at least once with both polarities. Some stimulation pairs were stimulated more often when time allowed this. We considered the responses to all stimuli in the analysis.

**Data pre-processing**

We excluded periods with burst suppression during the propofol-SPES because, in our set-up, it is an undesired state of the brain caused by too much propofol. We removed bad channels and periods with artefacts. Stimulation pairs or electrodes that met these exclusion criteria were excluded in both the clinical-SPES and propofol-SPES. The stimulation artefact [-1.5 ms: 9 ms] was replaced by the median value of the signal 20 ms before and after this interval. A low-pass, fourth-order Butterworth filter of 120 Hz was applied, as well as three fourth-order Butterworth band-stop filters (36 Hz, 50Hz and 110 Hz) to remove OR-related noise.

We determined an inter-observer agreement between two observers for the unfiltered clinical-SPES responses of two patients (PRIOS04 and PRIOS05). We used an unweighted Cohens kappa ($\kappa$) which was considered reasonable if $\kappa > 0.4$.

**Network characteristics**

We used an automatic detector to detect the N1-peak in each averaged response per electrode after stimulation of each stimulation pair [35], [54], [56]. We used the ERs to calculate the median and the Inter Quartile Range (IQR) of the overall, positive and negative agreement and the following network characteristics; the number of ERs evoked per stimulation pair, the in-degree per electrode, the out-degree per electrode and the BC per electrode. The in-degree, out-degree and BC were normalised by considering the number of stimulation pairs an electrode was part of, calculations are described in detail in *van Blooijs et al. (2018)* [23].

**ER-peak latencies**

The N1-peaks were visually checked for the responses and were corrected when an incorrect N1-peak was selected by the detector. The first positive peak found after the N1-peak and before $500\ ms$ was considered as the P1-peak, these were not visually checked. In PRIOS03, the median N2-latency was selected in signals that contained a confirmed N1. The manual selection of N2-peaks is time-consuming and was therefore performed for only one patient. The median N1-, P1- and N2-latencies were calculated using responses that contained an ER in both the clinical-SPES and the propofol-SPES.

**Statistical analysis**

We used the Wilcoxon Signed Rank test to compare the median of the absolute number of ERs evoked per stimulation pair, and to compare the median N1-, P1- and N2-latencies of the clinical-SPES and the propofol-SPES. We used the Spearman rank correlation to correlate the network characteristics between the clinical-SPES and the propofol-SPES. The strength of the correlation was expressed with the correlation coefficient ($r_s$).

We performed data pre-processing, calculations of the network characteristics and the statistical analysis using Matlab. The code is accessible on *https://github.com/SiefBlok/CCEP_NMM_SB/tree/master/CCEP/Prospective_analysis*. The RESPect dataset on https://openneuro.org/datasets/ds003399/versions/1.0.1 could be used to try the clinical script.

# Results

**Patient characteristics**

We included six patients (three females) with a median age of 33 years (range 12 – 53 years), see *Table 1*. SPES had been performed during the chronic clinical ECoG monitoring to evaluate the possibility of resective surgery for the treatment of their epilepsy at the Department of Clinical Neurophysiology in the University Medical Centre Utrecht in 2020. All patients were implanted with electrode strips and electrode grids (AdTech Medical Instruments Corp., WI, USA). PRIOS01 also had one depth-electrode. We found that the average time available to perform SPES in the OR, after the patient was anaesthetised with propofol and while surgical preparations were made, was 40 minutes (range 29-53 minutes).

**Inter-observer agreement**

For PRIOS04 we found an inter-observer agreement of $\kappa$ = 0.48 and for PRIOS05 we found a $\kappa$ of 0.55.

**Overall, positive and negative agreement**

The median overall agreement between the clinical-SPES and the propofol-SPES of all patients was 90% (IQR 82% – 93%). The median positive agreement of all patients was 53% (IQR 38% – 70%). The median negative agreement of all patients was 94% (range 90% – 96%).

***Table 1**: Characteristics of patients included in the PRIOS study.*

| Patient | Age | Gender | Location of grid |
|---|---|---|---|
| **PRIOS01** | 22 | M | Left temporal |
| **PRIOS02** | 53 | F | Left temporal |
| **PRIOS03** | 37 | M | Left frontal |
| **PRIOS04** | 24 | M | Left interhemispheric |
| **PRIOS05** | 51 | F | Right interhemispheric |
| **PRIOS06** | 12 | F | Right fronto-parietal |

**Absolute number of evoked ERs per stimulation pair**

PRIOS01, PRIOS04, PRIOS05 and PRIOS06 showed a significant decrease in the median number of ERs evoked per stimulation pair, see *Figure 2*. For all patients, the number of ERs evoked per stimulation pair found for the clinical-SPES was on average 3.8 times higher compared to the propofol-SPES (range 1 - 10 times more ERs during clinical-SPES).

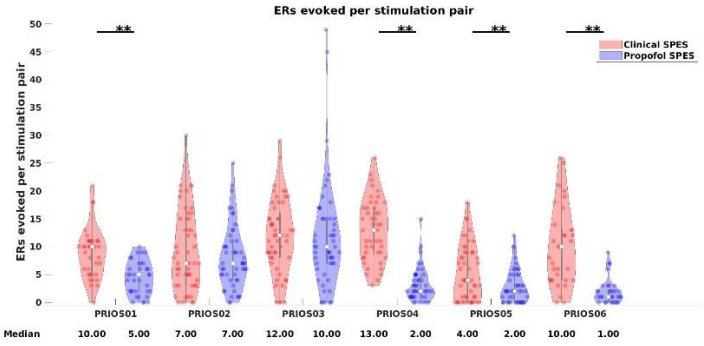


***Figure 2**: Number of ERs evoked per stimulation pair, in red the clinical-SPES and in blue the propofol-SPES. Each marker represents a stimulation pair. (** = p <0.001).*

**The network characteristics**

All patients except PRIOS01 and PRIOS04 showed a correlation for the ERs evoked per stimulation pair, the in-degree, the out-degree and the BC ($p < 0.05$, *Spearman*), see *Figure 3*. The value for the in-degree and the out-degree were on average 2.4 times higher for the clinical-SPES compared to the propofol-SPES. The BC of the clinical-SPES was 2.9 times higher compared to the propofol-SPES.

**ER-peak latencies**

PRIOS02, PRIOS03, PRIOS04 and PRIOS05 showed a significant increase of the median N1-latency during propofol-SPES. The median N1-latency during clinical-SPES for all patients was 22.7 ms (IQR 16.1 – 27.8 ms). The median N1-latency during propofol-SPES was 28.0 ms (IQR 13.7 – 29.3 ms). All patients showed an increase of the median P1-latency during propofol-SPES, except PRIOS06. The median P1-latency during clinical-SPES for all patients was 59.2 ms (IQR 53.0 – 60.5 ms). The median P1-latency during propofol-SPES for all patients was 65.7 ms (IQR 60.3 – 70.8 ms). For PRIOS03, we found a significant increase in the median N2-latency during propofol-SPES. The median latency during

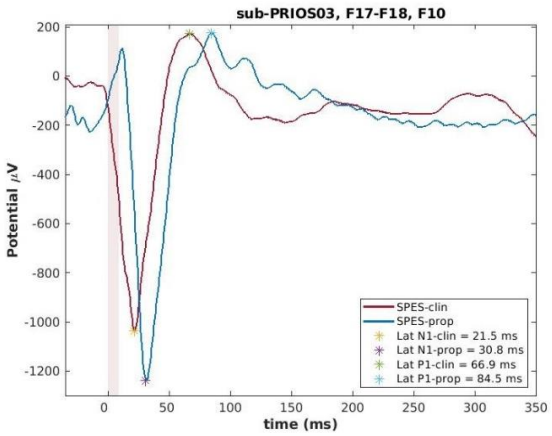


***Figure 4:** In red the averaged response during clinical-SPES and in blue the response for propofol-SPES. The N1- and P1-peaks are marked and the latencies are provided in the legend. The orange patch is the interval [-1.5 ms: 9ms] where interpolation is used around the stimulation artefact.*

clinical-SPES was 207,5 ms (IQR 181.8 – 266.2 ms), during propofol-SPES it was 219.7 ms (IQR 161.6 – 232.9 ms). *Figure 4* shows an example of increased latencies of the propofol-SPES for PRIOS03. Clinical examples of the other patients and Violin plots with the peak latencies are provided in *Appendix C*.

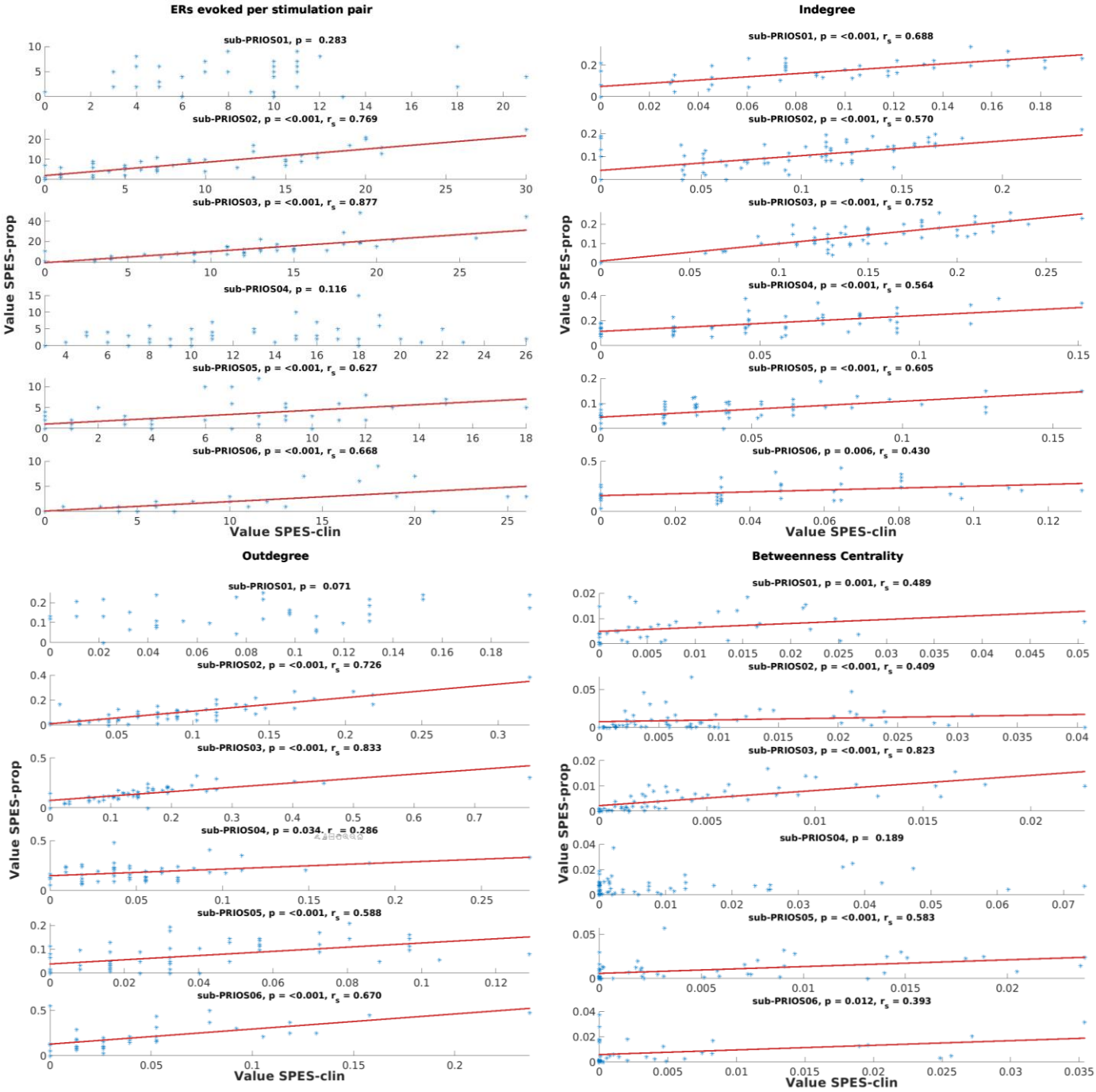


***Figure 3****: Scatter plots of the four network characteristics. Each marker represents a stimulation pair/electrode with on the x-axis its value for the clinical-SPES and on the y-axis its value for the propofol-SPES. The red line is the best fit through the data points. The correlation coefficient* ($r_s$) *is used to indicate the strength of the correlation.*

# Discussion

We studied whether SPES performed in propofol-anaesthetised patients showed the same neuronal connections compared to SPES as part of the clinical procedure. We hypothesised that the neuronal network based on the results of propofol-SPES would resemble the clinical-SPES. Though, propofol-SPES would result in a lower absolute number of evoked ERs and lead to increased latencies of the N1-, P1- and N2-peaks.

The results showed that the overall agreement between the clinical-SPES and the propofol-SPES is high, as well as the negative agreement. The median positive agreement is 53%. An explanation might be the low number of ERs in both datasets: a missing ER or false-negative scored response for the propofol-SPES could therefore cause a large decrease of the positive agreement. The absolute number of ERs evoked per stimulation pair during propofol-SPES is lower compared to clinical-SPES. PRIOS02 and PRIOS03 showed no significant difference between the absolute number of ERs evoked per stimulation pair of the clinical-SPES and the propofol-SPES. Nevertheless, all network characteristics showed a significant correlation for at least four out of the six patients. This indicated that propofol does not interfere with the functional connectivity of electrodes in a network based on evoked ERs. The lower absolute number of ERs evoked per stimulation pair during propofol-SPES complied with our hypothesis based on the inhibitory effect on neurotransmission.

The median N1-latency during clinical-SPES (22.5 $ms$) was comparable to the latency described by *Matsumoto et al. (2004)* [34]. It was lower than the latency found by *Enatsu et al. (2012)*, who found a median N1-latency of 60 ms [57]. However, they only applied electrical stimulation to the region of the ictal onset zone. During clinical-SPES, we found a median P1-latency of 59.6 $ms$. This is lower compared to the P1-latency reported by *Umeoka et al. (2009)* [58]. They reported a P1-latency of 93.4 ms. They reported a N1-latency that was already 40 $ms$ higher (63.2 ms) compared to the N1-latency we found. We did not perform a visual check of the detected P1-peaks which makes our results less reliable. The median N2-latency we found for PRIOS03 was 207.5 $ms$, this was larger than the N2-latency reported by *Matsumoto et al. (2004)* who reported a latency of 144.6 ms (range 113 - 164 ms) [34]. We only determined the N2-peak for PRIOS03 because the manual selection of the N2-peaks is a time-consuming task. To improve the reliability and the accuracy of the N2-latency, the N2-latencies should be determined in the other patients.

We found that the N1-, P1- and N2-latencies during propofol-SPES were significantly greater compared to clinical-SPES for four out of six patients. During propofol-SPES, we found a median increase of the N1-latency of 5.5 $ms$. This is much greater compared to the N1-latency difference reported by *Yamao et al. (2014)* who found a ± 0.7 $ms$ difference [28]. In their research, they compared SPES under general with SPES with local anaesthesia.

**Methodological issues**

Only ERs after 9 ms were detected by the detector. This is the earliest moment that electrodes can detect physiological responses [54]. We found that the N1-latency of PRIOS04 was often very close to the 9 ms limit or even less than 9 ms and therefore not detected by the detector. If all signals would be visually checked, then N1-peaks with a latency < 9 ms could be identified. However, that would be extremely time consuming and previous research concluded that the performance of the ER detector is sufficient for use in further research [54].

Above that, during this study, we filtered the data which was preceded by interpolation of the period [-1.5 – 9 $ms$]. Therefore even with visual inspection, we would not have been able to detect ERs <9 $ms$.

Future studies on propofol-SPES could focus on the value of the network characteristics of the electrodes on the EZ, for example, see *Figure 5. Van Blooijs et al. (2018)* [23] already found high in-degree and out-degree values on epileptogenic tissue of awake patients. In *Appendix B* we included a 2D grid visualisation of the network characteristics in which the seizure onset zone is indicated. We should keep in mind that propofol acts on the $\gamma$-aminobutyric acid receptor ($GABA_A$-receptor) [38]–[40]. It is precisely this $GABA_A$-receptor that is highly altered in epilepsy patients with a reduced number of $GABA_A$-receptors in the SOZ [59]–[63]. A future study could therefore investigate whether ECoG electrodes overlying epileptogenic tissue show a less prominent change of the network characteristics due to propofol.

From our retrospective study (*Chapter 2*) we concluded that 2 stimuli would suffice in forming a network similar to 10 stimuli. However, due to increased noise on the OR, it is recommended to use more than two stimuli per stimulation pair during propofol-SPES. This will increase the signal to noise ratio (SNR) that facilitates ER detection. Another recommendation to increase the SNR would be to re-reference by using a common average reference.

Based on the results described above, we conclude that performing SPES in propofol-anaesthetised epilepsy patients is feasible and that propofol does not interfere with the functional connectivity of electrodes in a network based on evoked ERs. For future studies, it is recommended to avoid the need to filter the signal because this has to be preceded by interpolation that leads to loss of data. Another recommendation would be to include more patients to generate higher reliability of the conclusion. More research is needed to be able to use propofol-SPES as a diagnostic tool for the localisation of the SOZ.

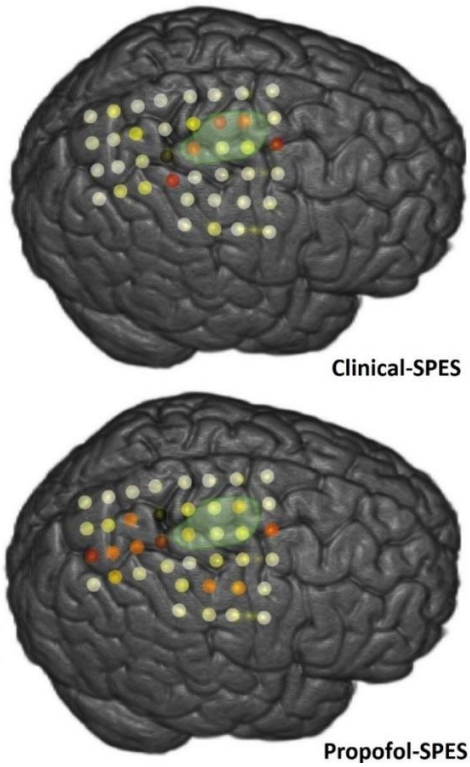


***Figure 5****: 2D grid visualisation of the BC of PRIOS06 for clinical-SPES and propofol-SPES. The SOZ is marked in green. The equal colouring of the electrodes shows that they had the same place on the ranking for both SPES sessions.*

# Chapter 4
# Analysis of a computational model

# Abstract

**Objective:** Propofol has an inhibitory effect on the neurotransmission of neuronal populations. In the previous chapter, we found increased N1- P1- and N2-latencies of the Early Responses (ER) during in vivo propofol-SPES. It is hypothesised that propofol caused this increase. We increased the activity of the inhibitory population in a Neural Mass Model (NMM) to study whether the hypothesised increase of latencies would occur in simulated ERs.

**Methods:** We used the default settings used by *Hebbink et al. (2020)* as a guideline to simulate the clinical- and propofol-SPES responses. To simulate the responses to clinical-SPES, we reduced the time constant of the slow inhibitory population ($b$) from 10 $s^{-1}$ to 4.6 $s^{-1}$. We also reduced the gain ($G$) and time constant ($g$) of the fast inhibitory population systematically and simultaneously. We varied $G$ from 10 to 25 $mV$, and $g$ from 145 $s^{-1}$ to 295 $s^{-1}$, with default settings of 25 $mV$ and 300 $s^{-1}$, respectively.

**Results:** Reducing the time constant $b$ resulted in an increase of the P1- and N2-latency. Reducing the gain ($G$) and time constant ($g$) of the fast inhibitory population increased the N1- and P1-peaks. We decided that simulations using a value for $G$ of 11 $mV$ and for $g$ of 175 $s^{-1}$ resulted in ER latencies that matched the latencies as found in our in vivo propofol-SPES study.

**Conclusion:** Increased activity of the fast inhibitory population led to increased peak latencies in the simulations. We conclude that an NMM with an adaptation of the fast inhibitory population suffices to explain the experimentally observed effect of propofol on an ECoG response.


# Background

**Modelling SPES responses**

An often-used Neural Mass Model (NMM) is the Wendling model [48]. The model simulates a single neural mass containing four neuronal populations, i.e., the pyramidal, excitatory, slow inhibitory and fast inhibitory population, see *Figure 4.1*. Pyramidal cells are considered the main population in the NMM [35], [48]. Due to their orientation perpendicular to the cortical surface and the fact that they can be activated simultaneously makes that pyramidal neurons are the main contributor to the electrical activity that is measured by EEG [49]. For this study, we used a variation to the Wendling model as suggested by *Hebbink et al. (2020)* [37]. They added feedforward inhibition to the model to study epileptiform ECoG responses to SPES.

Each population has a mean membrane potential, that is influenced by other populations or external inputs such as SPES. A synaptic transmission converts the activity or firing rate of the sending population/SPES into a postsynaptic potential (PSP) at the receiving population. A PSP can be modelled by a linear, second-order differential equation, see *Equation 4.1*. ERs can be modelled as (approximately) linear responses since the amplitude of ERs can be scaled linearly with the stimulation strength [2], [27], [35], [36].

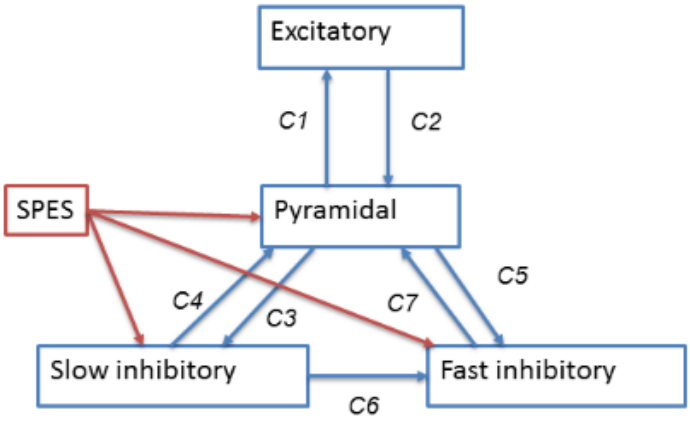


*Figure 4.1: Architecture of a single neural mass with the pyramidal population in the centre, surrounded by the excitatory population, the slow inhibitory population and the fast inhibitory population. SPES is represented here as an external input (red). The blue arrows represent connections between the populations with their connection strength parameters. This figure is adapted from Figure 4.11 of* [35].

$$\ddot{x}(t) = Qqz(t) - 2q\dot{x}(t) - q^2x(t) \tag{4.1}$$

In *Equation 4.1*, $Q$ is the synaptic gain that regulates the magnitude, and $1/q$ is the time constant of the synaptic response. Each population has its own parameter for $Q$ and $q$. The default values, by *Hebbink et al. (2020)* [37], are provided in *Table D1*. With these default settings, they found N1-, P1- and N2-latencies of $23\ ms$, $50\ ms$ and $118\ ms$, respectively.

ERs can be used to reveal the neural network [23]. In the future, the ECoG responses of a whole network could be simulated by coupled-NMMs. A surgical strategy might be proposed based on virtual resections of NMMs [16]. As current research with SPES relies on un-anaesthetised patients, we want to study the effect of propofol on SPES. In the in vivo study described in the previous chapter, we found increased latencies of the N1-, P1- and N2-peak during SPES performed in propofol-anaesthetised patients, see *Table 4.1* and *Figure C.2* in *Appendix C*. *Hindriks & van Putten (2012)* reported that the effect of propofol on the EEG could be simulated by decreasing the time constant of the inhibitory populations [41]. In this sub-study, we aimed to simulate the effect of propofol on an ECoG response to SPES by adapting the parameters of the inhibitory populations in an NMM. These simulations could explain the observed peak differences of ERs in agreement with the known inhibitory effect of propofol.

*Table 4.1: The median N1-, P1-latency during clinical-SPES and propofol-SPES of six patients (Chapter 3). The median N2-latency of one patient. All three peak latencies increase during propofol-SPES.*

| | **Clinical-SPES (ms)** | **Propofol-SPES (ms)** |
|---|---|---|
| **N1** | 22.7 (IQR 16.1 – 27.8) | 28.0 (IQR 13.7 – 29.3) |
| **P1** | 59.2 (IQR 53.0 – 60.5) | 65.7 (IQR 60.3 – 70.8) |
| **N2** | 207.5 (IQR 181.8 – 266.2) | 219.7 (IQR 161.6 – 232.9) |

# Method

**Modelling clinical-SPES**

We used the model as described by *Hebbink et al. (2020)* [16], [37]. We did not use the coupled second NMM. We minimised the noise from the simulations by a factor of 0.001. We did this to be able to study the basic effects on the ER-peak latencies. The model already produced ERs as a response to a clinical-SPES setting. We used the default settings used by *Hebbink et al. (2020)* as a guideline to model the clinical-SPES. These default values are provided in *Table D1* in *Appendix D*. During our in vivo study we found larger P1- and N2-latencies compared to the values documented by *Hebbink et al. (2020)* [37]. We reduced the time constant $(b)$ of the slow inhibitory population to increase the P1- and N2-latency as a response to clinical-SPES.

**Modelling propofol-SPES**

We used the clinical-SPES settings as described in the paragraph above, with $b$ set at 4.6 $s^{-1}$. We used the default values for all other parameters, as suggested by *Hebbink et al. (2020)*. After an initial sensitivity analysis, we reduced the gain $G$ and time constant $g$ systematically and simultaneously. We varied $G$ from 10 to 50 $mV$, and $g$ from 145 $s^{-1}$ – 400 $s^{-1}$, with default settings of 25 $mV$ and 300 $s^{-1}$, respectively. We found that settings with a gain $(G)$ or time constant $(g)$ higher than the default setting did not decrease the peak latencies. This is why we only studied the results of settings with a lower gain and time constant than the default. We chose a combination of the gain and time constant that resulted in at least two of the desired peak latencies as found during our in vivo study.

We performed data pre-processing, calculations of the ER-peak latencies and the statistical analysis using Matlab. The code will be openly available on *https://github.com/SiefBlok/CCEP_NMM_SB/tree/master/CCEP/Prospective_analysis* and *https://github.com/SiefBlok/CCEP_NMM_SB/tree/master/NMM* after publication.

# Results

**Simulate Clinical-SPES**

Reducing the time constant of the slow inhibitory population $(b)$ resulted in a better match with the P1- and N2-latency as found during the clinical-SPES of our in vivo study, see *Figure 4.2*. It did not increase the latency nor the amplitude of the N1-peak.

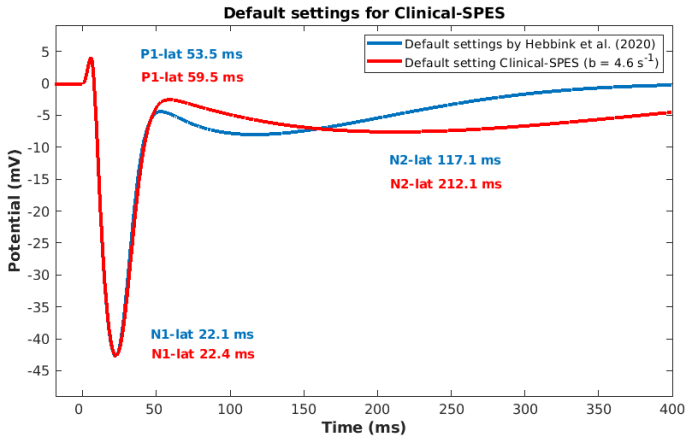


*Figure 4.2: In blue the simulated ERs for the default setting used by Hebbink et al. (2020) ($b = 10\ s^{-1}$). In red the simulated ER with a decreased time constant of the slow inhibitory population ($b = 4.6\ s^{-1}$). The P1- and N2-peak latency better matched the latencies as found during our in vivo study.*

**Simulate Propofol-SPES**

Decreasing the time constant for the fast inhibitory population $(g)$ led to an increase of the latency of the N1-, P1- and N2-peak, see *Figure 4.3* and *Figure D4.3* in *Appendix D*. It can also be seen that reducing the time constant did not influence the N2-latency for values $G < 21\ mV$. Setting the time constant $(g)$ lower than 145 $s^{-1}$ did not result in more combinations of the desired latency of all three peaks.

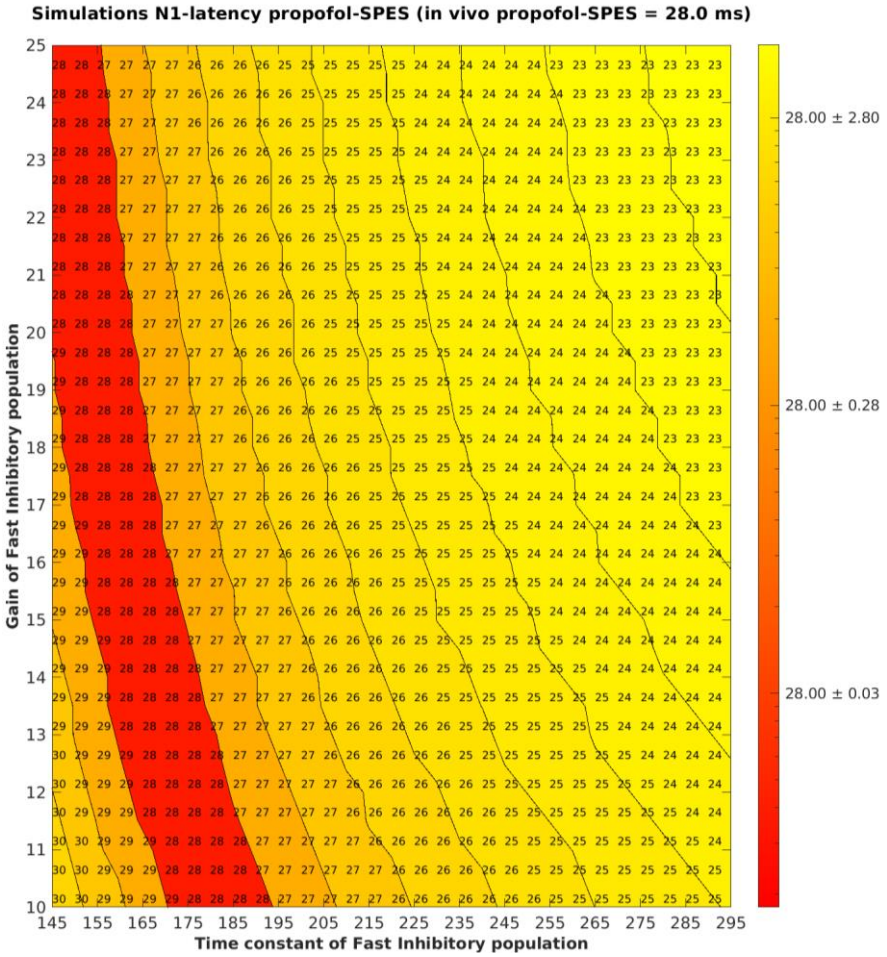


*Figure 4.3: Figure continues on next page*

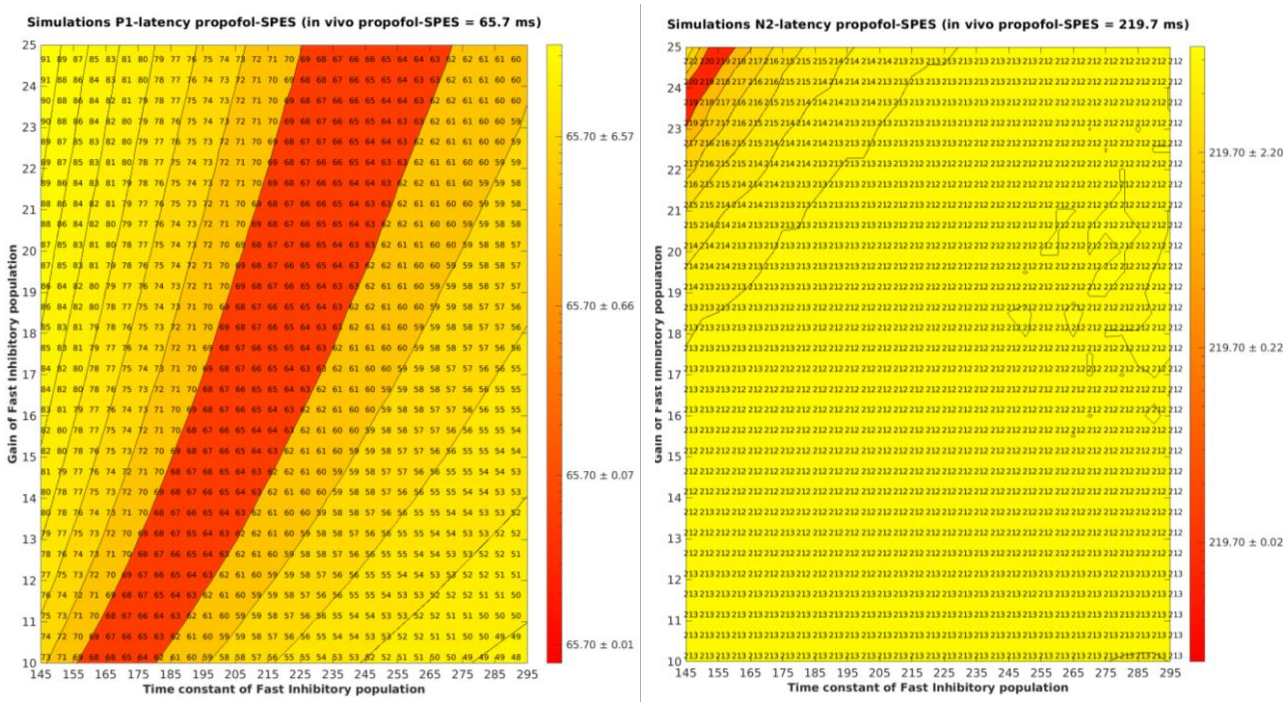


*Figure 4.3: Contour plot of the N1-, P1- and N2-latencies for values of the fast inhibitory population. On each x-axis, the value for the time constant, on each y-axis, the values for the gain. The desired peak latency, as found during the in vivo experiment, is provided in the title. Each time constant and gain setting that results in the desired latency is shown in red. A logarithmic scale is used to display the deviation from the desired latency.*

We found multiple gain and time constant settings that were able to simulate an ER with either the desired latencies for the N1-, P1- or the N2-peak. We decided that simulations using a value for $G$ of 11 $mV$ and for $g$ of 175 $s^{-1}$ resulted in ER latencies that matched the N1- and P1-latency as found in our in vivo propofol-SPES study, see *Figure 4.4*. The N2-latency was lower compared to the latency found during our in vivo study. The N2-latency of the simulated propofol-SPES response was equal to the N2-latency of the simulated clinical-SPES response. *Figure 4.4* shows that the amplitude of the N1-peak for the propofol-SPES simulation was much smaller compared to the amplitude of the clinical-SPES.

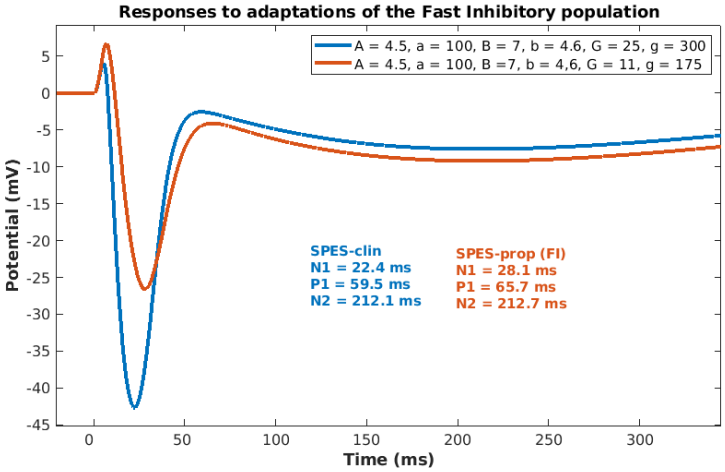


*Figure 4.4: Simulated responses for the clinical-SPES (blue) and for the propofol-SPES (orange) by adaptations of the gain ($G$) and the time constant ($g$) of the fast inhibitory population, see the legend.*

# Discussion

In this study, we aimed to simulate the effect of propofol on an ER by adapting the parameters of the inhibitory populations in an NMM. We used these simulations to explain the observed peak differences of ERs in agreement with the known inhibitory effect of propofol. We confirmed our hypothesis of increased N1-, P1-latencies when decreasing the gain and time constant of the fast inhibitory populations. We simulated an ER for which the N1-, P1-peak latencies were similar to the results found in our in vivo study.

Not much was known about a physiological range for the NMM-settings required to simulate the effect of propofol on SPES responses. Nevertheless, *Hindriks & van Putten (2012)* reported that reducing the decay rate of the action of the inhibitory population led to prolongation of the effect on EEG phenomenology [41]. We used a smaller value for the time constant of the slow inhibitory populations ($b$) compared to *Hebbink et al. (2020)* [37]. This resulted in a better match with the P1- and N2-latency as found during the clinical-SPES of our in vivo study. For the original model by *Wendling et al. (2002),* a much higher value for the gain of the fast inhibitory population, and much lower values for the slow inhibitory population were used [48]. *Ferrat et al. (2018)* [64] reported the widest ranges of parameter values used in theoretical studies that simulated physiological EEG. Our settings for the gain of each population, for the clinical-SPES and propofol-SPES simulations, were within the mentioned physiological range. The values of the time constant of the fast and slow inhibitory population were lower compared to the mentioned range. A reason for the deviation from *Wendling et al. (2002),* and the values reported in *Ferrat et al. (2018),* could be that they used the model to study high-frequency EEG activity and other epileptiform rhythms. While we used the model to study SPES responses recorded in subdural EEG, with and without the influence of propofol.

**Methodological issues**

We found that the N1-amplitude of the clinical-SPES simulation was larger compared to the N1-amplitude of the propofol-SPES simulation. Maintaining the amplitude, by using a higher gain ($G$) for the propofol-SPES simulation, did not result in a combination of the desired N1- and P1-latencies for the propofol-SPES. *Hindriks & van Putten (2012)* mentioned that the peak-amplitude of the EEG was not influenced by propofol [41]. ERs can be thought of as a direct, linear response to stimulation which is why we did not consider the magnitude of the amplitude as a criterion for the value of the population parameters. Moreover, we were not able to determine the amplitudes of the peaks during our in vivo experiments. Therefore we did not have a guideline to set the amplitude in the simulations.

A limitation of this study is that we minimised noise in our simulations to be able to study the basic effects on the ER-peak latencies. Noise could be used to represent background input from unmodeled brain regions. As a result, different peak latencies will be found while the same settings are used. This

would lead to simulations that are more comparable with the in vivo measurements. When studying simulations of delayed responses to SPES on epilepsy patients simulations must include noise. Noise pushes the model only occasionally beyond a threshold for generating delayed responses [16].

The latency of the P1-peak was of great importance for selecting the right gain and time constant combination. However, no visual check was performed on the selected P1-peaks during our in vivo experiments. We would recommend, for future experiments, to perform a visual check of these P1-peaks, similar to the visual check of the N1-peaks. For this study, the desired N2-latency from the in vivo experiments was based on one patient. Therefore, the N2-latency had less influence on the final NMM parameter values. Calculating a median N2-latency of more patients would improve the reliability and accuracy of this setting. For future research, it would be interesting to study combinations of time constants of the slow and fast inhibitory population to find an optimal setting to simulate the desired N1-, P1- as well as the N2-latency. Finally, we recommend including noise in the simulations of the clinical-SPES and propofol-SPES responses. This would lead to simulations more closely related to the observed responses of the in vivo measurements.

We conclude that an NMM with an adaptation of the inhibitory population suffices to explain the experimentally observed effect of propofol on an ECoG response.

# Chapter 5
# General discussion and general conclusion

In this research, we tried to take the first step towards making the invasive monitoring period for epilepsy patients redundant. We studied the possibility to perform SPES intra-operatively. Due to limited time to perform SPES in the OR, we first determined whether we could use a subset of 2 stimuli per stimulation pair to obtain a network with the same functional connectivity as a network based on 10 stimuli per stimulation pair (see *Chapter 2*). Traditionally, each stimulation pair is stimulated 10 times to be able to detect DRs despite their stochastic behaviour. ERs occur consistently and 2 stimuli per stimulation pair would therefore suffice in an analysis based on ERs. We found that fewer ERs were evoked per stimulation pair in the 2 stimuli setting. We found a median positive agreement of 71%, the in-degree, out-degree and BC, based on ERs, showed a significant correlation between the 10 stimuli setting and the 2 stimuli setting for five out of the six patients. This implied that electrodes had the same function and importance within the network of both settings. A point of improvement of this study described in *Chapter 2* would be to visually check the automatically detected ERs.

In *Chapter 3*, we compared the networks derived from clinical-SPES with the networks derived from the intra-operative SPES for six patients. We determined the same network characteristics as calculated in *Chapter 2*, as well as the latency of the N1-, P1- and N2-peaks. We found that fewer ERs were evoked per stimulation pair during the propofol-SPES. We found a median positive agreement of 53% and the in-degree, out-degree and BC, based on ERs, showed a significant correlation for at least four out of the six patients. We found significant differences for the N1-, P1- and N2-latencies of the responses to in vivo propofol-SPES compared to clinical-SPES. We concluded that performing SPES in propofol-anaesthetised epilepsy patients is feasible and that propofol does not interfere with the function and importance of electrodes in a network based on ERs. For future studies, it is recommended to avoid the need to filter the signal because this has to be preceded by interpolation that leads to loss of data. Another recommendation would be to include more patients to generate higher reliability of the conclusion. It is also recommended to increase the signal to noise ratio to facilitate ER detection. This could be managed by using more than two stimuli per stimulation pair during propofol-SPES or by re-referencing with a common average reference.

In *Chapter 4*, we used an NMM with adaptations of the inhibitory populations to simulate the experimentally observed effect of propofol on ERs. We hypothesised that propofol would prolong the action of the inhibitory populations. This leads to increased peak latencies of an ER. We were able to find parameter settings for the NMM to simulate the increased peak latencies as found during our in vivo experiments. We concluded that an NMM with adaptations of the inhibitory populations suffices to invoke the in vivo observed effect of propofol on an ECoG response.

The strength of this study is that it was the first study to compare the neural network derived from SPES in a propofol-anaesthetised patient with the network derived from SPES performed while that patient was in a state of relaxed awareness during chronic ECoG monitoring. In addition to that, we were able to use an NMM with adaptations of the inhibitory populations to simulate a response to propofol-SPES.

We were able to include six patients in this study. We are allowed by the ethical committee of the University Medical Centre of Utrecht to include patients up until June 2022, or a maximum of 20 patients. Studying the results of more patients could lead to more knowledge about the effect of propofol on the neuronal networks found by SPES and hopefully strengthen the conclusions drawn so far.

For future studies, we would be interested to focus on the different effects of propofol on electrodes in or outside the SOZ. The $GABA_A$-receptor is altered in epilepsy patients with a reduced number of $GABA_A$-receptors in the SOZ. Electrodes located on the SOZ could therefore be less affected by propofol. The degree of influence of propofol (e.g. a certain increase of N1-latency) might be used as an indicator of the SOZ.

# References


[1] C. E. Stafstrom and L. Carmant, "Seizures and epilepsy: An overview for neuroscientists," *Cold Spring Harb. Perspect. Biol.*, vol. 7, no. 5, pp. 1–19, 2015, doi: 10.1101/cshperspect.a022426.

[2] A. Valentín *et al.*, "Responses to single pulse electrical stimulation identify epileptogenesis in the human brain in vivo," *Brain*, vol. 125, no. 8, pp. 1709–1718, Aug. 2002, doi: 10.1093/brain/awf187.

[3] A. Valentín *et al.*, "Single pulse electrical stimulation for identification of structural abnormalities and prediction of seizure outcome after epilepsy surgery: A prospective study," *Lancet Neurol.*, vol. 4, no. 11, pp. 718–726, Nov. 2005, doi: 10.1016/S1474-4422(05)70200-3.

[4] J. Žiburkus, J. R. Cressman, and S. J. Schiff, "Seizures as imbalanced up states: Excitatory and inhibitory conductances during seizure-like events," *J. Neurophysiol.*, vol. 109, no. 5, pp. 1296–1306, 2013, doi: 10.1152/jn.00232.2012.

[5] Volksgezondheidenzorg.info, "Epilepsie | Cijfers & Context | Trends." https://www.volksgezondheidenzorg.info/onderwerp/epilepsie/cijfers-context/trends#node-trend-prevalentie-epilepsie (accessed Feb. 15, 2021).

[6] Epilepsiefonds, "Epilepsiechirurgie - Over epilepsie." https://www.epilepsie.nl/over-epilepsie/pagina/101-2/epilepsiechirurgie/ (accessed Mar. 23, 2021).

[7] J. De Tisi *et al.*, "The long-term outcome of adult epilepsy surgery, patterns of seizure remission, and relapse: A cohort study," *Lancet*, vol. 378, no. 9800, pp. 1388–1395, Oct. 2011, doi: 10.1016/S0140-6736(11)60890-8.

[8] J. Engel, "Progress in the field of epilepsy," *Current Opinion in Neurology*, vol. 26, no. 2. pp. 160–162, Apr. 2013, doi: 10.1097/WCO.0b013e32835ee5a3.

[9] B. C. Jobst and G. D. Cascino, "Resective epilepsy surgery for drug-resistant focal epilepsy: A review," *JAMA - J. Am. Med. Assoc.*, vol. 313, no. 3, pp. 285–293, Jan. 2015, doi: 10.1001/jama.2014.17426.

[10] S. G. Uijl *et al.*, "Epilepsy surgery can help many more adult patients with intractable seizures," *Epilepsy Res.*, vol. 101, no. 3, pp. 210–216, Sep. 2012, doi: 10.1016/j.eplepsyres.2012.04.002.

[11] H. J. Lamberink *et al.*, "Seizure outcome and use of antiepileptic drugs after epilepsy surgery according to histopathological diagnosis: a retrospective multicentre cohort study," *Lancet Neurol.*, vol. 19, no. 9, pp. 748–757, Sep. 2020, doi: 10.1016/S1474-4422(20)30220-9.

[12] M.-C. Picot, M. Baldy-Moulinier, J.-P. Daurs, P. Dujols, and A. Crespel, "The prevalence of epilepsy and pharmacoresistant epilepsy in adults: A population-based study in a Western European country," *Epilepsia*, vol. 49, no. 7, pp. 1230–1238, Jul. 2008, doi: 10.1111/j.1528-1167.2008.01579.x.

[13] H. Lüders, I. Awad, R. Burgess, E. Wyllie, and P. Van Ness, "Subdural electrodes in the presurgical evaluation for surgery of epilepsy," *Epilepsy Res. Suppl.*, vol. 5, p. 147—156, 1992, [Online]. Available: http://europepmc.org/abstract/MED/1418444.

[14] L. Jehi, "The epileptogenic zone: Concept and definition," *Epilepsy Currents*, vol. 18, no. 1. American Epilepsy Society, pp. 12–16, Jan. 01, 2018, doi: 10.5698/1535-7597.18.1.12.

[15] F. Rosenow and H. Lüders, "Presurgical evaluation of epilepsy," *Brain*, vol. 124, no. 9, pp. 1683–1700, Sep. 2001, doi: 10.1093/brain/124.9.1683.

[16] J. Hebbink, H. Meijer, G. Huiskamp, S. van Gils, and F. Leijten, "Phenomenological network models: Lessons for epilepsy surgery," *Epilepsia*, vol. 58, no. 10, pp. e147–e151, Oct. 2017, doi: 10.1111/epi.13861.

[17] S. S. Spencer, "Neural networks in human epilepsy: Evidence of and implications for treatment," *Epilepsia*, vol. 43, no. 3, pp. 219–227, 2002, doi: 10.1046/j.1528-1157.2002.26901.x.

[18] E. G. Neal, S. Maciver, M. R. Schoenberg, and F. L. Vale, "Surgical disconnection of epilepsy network correlates with improved outcomes," *Seizure*, vol. 76, pp. 56–63, Mar. 2020, doi: 10.1016/j.seizure.2020.01.018.

[19] M. Zijlmans, G. M. Huiskamp, O. L. Cremer, C. H. Ferrier, A. C. Van Huffelen, and F. S. S. Leijten, "Epileptic high-frequency oscillations in intraoperative electrocorticography: The effect of propofol," *Epilepsia*, vol. 53, no. 10, pp. 1799–1809, Oct. 2012, doi: 10.1111/j.1528-1167.2012.03650.x.

[20] J. D. Rolston, "Surgical Strategies for Epilepsy in Eloquent Areas," *Epilepsy J.*, vol. 02, no. 01,

2015, doi: 10.4172/2472-0895.1000103.
[21] A. Kuruvilla and R. Flink, “Intraoperative electrocorticography in epilepsy surgery: Useful or not?,” *Seizure*, vol. 12, no. 8, pp. 577–584, Dec. 2003, doi: 10.1016/S1059-1311(03)00095-5.
[22] R. P. Lesser, N. E. Crone, and W. R. S. Webber, “Subdural electrodes,” *Clinical Neurophysiology*, vol. 121, no. 9. Elsevier, pp. 1376–1392, Sep. 01, 2010, doi: 10.1016/j.clinph.2010.04.037.
[23] D. van Blooijs, F. S. S. Leijten, P. C. van Rijen, H. G. E. Meijer, and G. J. M. Huiskamp, “Evoked directional network characteristics of epileptogenic tissue derived from single pulse electrical stimulation,” *Hum. Brain Mapp.*, vol. 39, no. 11, pp. 4611–4622, Nov. 2018, doi: 10.1002/hbm.24309.
[24] “Invasive electroencephalography (EEG) monitoring before epilepsy surgery.” https://www.aboutkidshealth.ca/Article?contentid=2056&language=English (accessed Sep. 24, 2020).
[25] M. A. van ’t Klooster, M. Zijlmans, F. S. S. Leijten, C. H. Ferrier, M. J. A. M. van Putten, and G. J. M. Huiskamp, “Time–frequency analysis of single pulse electrical stimulation to assist delineation of epileptogenic cortex,” *Brain*, vol. 134, no. 10, pp. 2855–2866, Oct. 2011, doi: 10.1093/brain/awr211.
[26] B. E. Mouthaan *et al.*, “Single Pulse Electrical Stimulation to identify epileptogenic cortex: Clinical information obtained from early evoked responses,” *Clin. Neurophysiol.*, vol. 127, no. 2, pp. 1088–1098, Feb. 2016, doi: 10.1016/j.clinph.2015.07.031.
[27] R. Enatsu *et al.*, “Cortical excitability varies upon ictal onset patterns in neocortical epilepsy: A cortico-cortical evoked potential study,” *Clin. Neurophysiol.*, vol. 123, no. 2, pp. 252–260, Feb. 2012, doi: 10.1016/j.clinph.2011.06.030.
[28] Y. Yamao *et al.*, “Intraoperative dorsal language network mapping by using single-pulse electrical stimulation,” *Hum. Brain Mapp.*, vol. 35, no. 9, pp. 4345–4361, 2014, doi: 10.1002/hbm.22479.
[29] R. Matsumoto, T. Kunieda, and D. Nair, “Single pulse electrical stimulation to probe functional and pathological connectivity in epilepsy,” *Seizure*, vol. 44. W.B. Saunders Ltd, pp. 27–36, Jan. 01, 2017, doi: 10.1016/j.seizure.2016.11.003.
[30] R. Matsumoto, D. R. Nair, E. LaPresto, W. Bingaman, H. Shibasaki, and H. O. Luders, “Functional connectivity in human cortical motor system: a cortico-cortical evoked potential study,” *Brain*, vol. 130, no. 1, pp. 181–197, Nov. 2006, doi: 10.1093/brain/awl257.
[31] A. Valentin and G. Alarcon, “Single Pulse Electrical Stimulation in Presurgical Assessment of Epilepsy: A New Diagnostic Tool,” *Adv Clin Neurosci Rehabil*, vol. 8, pp. 14–18, Jan. 2008, Accessed: Oct. 09, 2020. [Online]. Available: https://www.acnr.co.uk/mar_apr_2008/ACNRMA08_single.pdf.
[32] G. Alarcón and A. Valentín, “Cortical stimulation with single electrical pulses in human epilepsy,” *Clinical Neurophysiology*, vol. 123, no. 2. Clin Neurophysiol, pp. 223–224, Feb. 2012, doi: 10.1016/j.clinph.2011.07.001.
[33] V. Kokkinos, G. Alarcón, R. P. Selway, and A. Valentín, “Role of single pulse electrical stimulation (SPES) to guide electrode implantation under general anaesthesia in presurgical assessment of epilepsy,” *Seizure*, vol. 22, no. 3, pp. 198–204, Apr. 2013, doi: 10.1016/j.seizure.2012.12.012.
[34] R. Matsumoto *et al.*, “Functional connectivity in the human language system: A cortico-cortical evoked potential study,” *Brain*, vol. 127, no. 10, pp. 2316–2330, Oct. 2004, doi: 10.1093/brain/awh246.
[35] J. Hebbink, “Computational Modelling and Electrical Stimulation for Epilepsy Surgery - PhD Thesis,” 2019, doi: 10.3990/1.9789036548328.
[36] G. Alarcón, D. Jiménez-Jiménez, A. Valentín, and D. Martín-López, “Characterizing EEG Cortical Dynamics and Connectivity with Responses to Single Pulse Electrical Stimulation (SPES),” *Int. J. Neural Syst.*, vol. 13, no. 6, p. 1750057, 2018, doi: 10.1142/S0129065717500575.
[37] J. Hebbink, G. Huiskamp, and S. A. van Gils, “Pathological responses to single-pulse electrical stimuli in epilepsy: The role of feedforward inhibition,” *Eur. J. Neurosci.*, vol. 51, no. 4, pp. 1122–1136, Sep. 2020, doi: 10.1111/ejn.14562.

[38] M. M. Sahinovic, M. M. R. F. Struys, and A. R. Absalom, “Clinical Pharmacokinetics and Pharmacodynamics of Propofol,” *Clinical Pharmacokinetics*, vol. 57, no. 12. Springer International Publishing, pp. 1539–1558, Dec. 01, 2018, doi: 10.1007/s40262-018-0672-3.
[39] U. Rudolph and B. Antkowiak, “Molecular and neuronal substrates for general anaesthetics,” *Nature Reviews Neuroscience*, vol. 5, no. 9. Nat Rev Neurosci, pp. 709–720, Sep. 2004, doi: 10.1038/nrn1496.
[40] G. M. S. Yip *et al.*, “A propofol binding site on mammalian GABA A receptors identified by photolabeling,” *Nat. Chem. Biol.*, vol. 9, no. 11, pp. 715–720, Nov. 2013, doi: 10.1038/nchembio.1340.
[41] R. Hindriks and M. J. A. M. van Putten, “Meanfield modeling of propofol-induced changes in spontaneous EEG rhythms,” *Neuroimage*, vol. 60, no. 4, pp. 2323–2334, May 2012, doi: 10.1016/j.neuroimage.2012.02.042.
[42] F. Wendling, “Computational models of epileptic activity: A bridge between observation and pathophysiological interpretation,” *Expert Review of Neurotherapeutics*, vol. 8, no. 6. Future Drugs Ltd, pp. 889–896, 2008, doi: 10.1586/14737175.8.6.889.
[43] F. Wendling, P. Benquet, F. Bartolomei, and V. Jirsa, “Computational models of epileptiform activity,” *Journal of Neuroscience Methods*, vol. 260. Elsevier, pp. 233–251, Feb. 15, 2016, doi: 10.1016/j.jneumeth.2015.03.027.
[44] S. N. Kalitzin, D. N. Velis, and F. H. Lopes da Silva, “Stimulation-based anticipation and control of state transitions in the epileptic brain,” *Epilepsy Behav.*, vol. 17, no. 3, pp. 310–323, Mar. 2010, doi: 10.1016/j.yebeh.2009.12.023.
[45] O. Benjamin *et al.*, “A phenomenological model of seizure initiation suggests network structure may explain seizure frequency in idiopathic generalised epilepsy,” *J. Math. Neurosci.*, vol. 2, no. 1, p. 1, 2012, doi: 10.1186/2190-8567-2-1.
[46] O. David and K. J. Friston, “A neural mass model for MEG/EEG: Coupling and neuronal dynamics,” *Neuroimage*, vol. 20, no. 3, pp. 1743–1755, Nov. 2003, doi: 10.1016/j.neuroimage.2003.07.015.
[47] M. A. Whittington, R. D. Traub, N. Kopell, B. Ermentrout, and E. H. Buhl, “Inhibition-based rhythms: Experimental and mathematical observations on network dynamics,” in *International Journal of Psychophysiology*, 2000, vol. 38, no. 3, pp. 315–336, doi: 10.1016/S0167-8760(00)00173-2.
[48] F. Wendling, F. Bartolomei, J. J. Bellanger, and P. Chauvel, “Epileptic fast activity can be explained by a model of impaired GABAergic dendritic inhibition,” *Eur. J. Neurosci.*, vol. 15, no. 9, pp. 1499–1508, May 2002, doi: 10.1046/j.1460-9568.2002.01985.x.
[49] T. Kirschstein and R. Köhling, “What is the source of the EEG?,” *Clin. EEG Neurosci.*, vol. 40, no. 3, pp. 146–149, 2009, doi: 10.1177/155005940904000305.
[50] T. L. Eissa *et al.*, “Cross-scale effects of neural interactions during human neocortical seizure activity,” *Proc. Natl. Acad. Sci. U. S. A.*, vol. 114, no. 40, pp. 10761–10766, Oct. 2017, doi: 10.1073/pnas.1702490114.
[51] S. Olmi, S. Petkoski, M. Guye, F. Bartolomei, and V. Jirsa, “Controlling seizure propagation in large-scale brain networks,” *PLOS Comput. Biol.*, vol. 15, no. 2, p. e1006805, Feb. 2019, doi: 10.1371/journal.pcbi.1006805.
[52] M. Rubinov and O. Sporns, “Complex network measures of brain connectivity: Uses and interpretations,” *Neuroimage*, vol. 52, no. 3, pp. 1059–1069, Sep. 2010, doi: 10.1016/j.neuroimage.2009.10.003.
[53] D. Van Blooijs *et al.*, “A practical workflow for organizing clinical intracranial EEG data in the intraoperative and long term monitoring settings in the Brain Imaging Data Structure. Pre-print,” doi: 10.1101/2020.12.07.20245290.
[54] D. van Blooijs, “Improving the SPES protocol by automating ER and DR detection and evaluation of the spatial relation between ERs and DRs - MSc Thesis,” University of Twente, Enschede, 2015.
[55] D. L. Keene, S. Whiting, and E. C. G. Ventureyra, “Electrocorticography,” *Epileptic Disord.*, vol. 2, no. 1, pp. 57–64, Apr. 2000, Accessed: Dec. 14, 2020. [Online]. Available: http://www.jle.com/fr/revues/epd/e-docs/electrocorticography_110192/article.phtml?tab=texte.
[56] J. Hebbink, D. van Blooijs, G. Huiskamp, F. S. S. Leijten, S. A. van Gils, and H. G. E. Meijer,

"A Comparison of Evoked and Non-evoked Functional Networks," *Brain Topogr.*, vol. 32, no. 3, pp. 405–417, May 2019, doi: 10.1007/s10548-018-0692-1.

[57] R. Enatsu *et al.*, "Correlations between ictal propagation and response to electrical cortical stimulation: A cortico-cortical evoked potential study," *Epilepsy Res.*, vol. 101, no. 1–2, pp. 76–87, Aug. 2012, doi: 10.1016/j.eplepsyres.2012.03.004.

[58] S. Umeoka *et al.*, "Neural connection between bilateral basal temporal regions: Cortico-cortical evoked potential analysis in patients with temporal lobe epilepsy," in *Neurosurgery*, May 2009, vol. 64, no. 5, pp. 847–855, doi: 10.1227/01.NEU.0000344001.26669.92.

[59] G. Sperk, S. Furtinger, C. Schwarzer, and S. Pirker, "GABA and its receptors in epilepsy," *Advances in Experimental Medicine and Biology*, vol. 548. Kluwer Academic/Plenum Publishers, pp. 92–103, 2004, doi: 10.1007/978-1-4757-6376-8_7.

[60] A. Avendaño-Estrada *et al.*, "Quantitative Analysis of [18F]FFMZ and [18F]FDG PET Studies in the Localization of Seizure Onset Zone in Drug-Resistant Temporal Lobe Epilepsy," *Stereotact. Funct. Neurosurg.*, vol. 97, no. 4, pp. 232–240, Dec. 2019, doi: 10.1159/000503692.

[61] S. Zhu, C. M. Noviello, J. Teng, R. M. Walsh, J. J. Kim, and R. E. Hibbs, "Structure of a human synaptic GABAA receptor," *Nature*, vol. 559, no. 7712, pp. 67–88, Jun. 2018, doi: 10.1038/s41586-018-0255-3.

[62] A. Galanopoulou, "GABAA Receptors in Normal Development and Seizures: Friends or Foes?," *Curr. Neuropharmacol.*, vol. 6, no. 1, pp. 1–20, Mar. 2008, doi: 10.2174/157015908783769653.

[63] F. Loup, H. G. Wieser, Y. Yonekawa, A. Aguzzi, and J. M. Fritschy, "Selective alterations in GABA(A) receptor subtypes in human temporal lobe epilepsy," *J. Neurosci.*, vol. 20, no. 14, pp. 5401–5419, Jul. 2000, doi: 10.1523/jneurosci.20-14-05401.2000.

[64] L. A. Ferrat, M. Goodfellow, and J. R. Terry, "Classifying dynamic transitions in high dimensional neural mass models: A random forest approach," *PLoS Comput. Biol.*, vol. 14, no. 3, p. e1006009, Mar. 2018, doi: 10.1371/journal.pcbi.1006009.

# Appendix A:

The 2D grid visualisation of the network characteristics of all patients of the retrospective analysis in *Chapter 2*. Different scales for the colour bar were used to show that the electrodes with the highest value in the setting with 10 stimuli still had the highest value in the setting with 2 stimuli. We used a representation of the patient's grid as close to reality as possible. The distance between each electrode on the same grid is in reality equal in the length and width of the grid. The distance between individual grids could deviate from the visualisation below. An improvement would be to group the electrodes that are on the same gyrus.

**A**

**B**

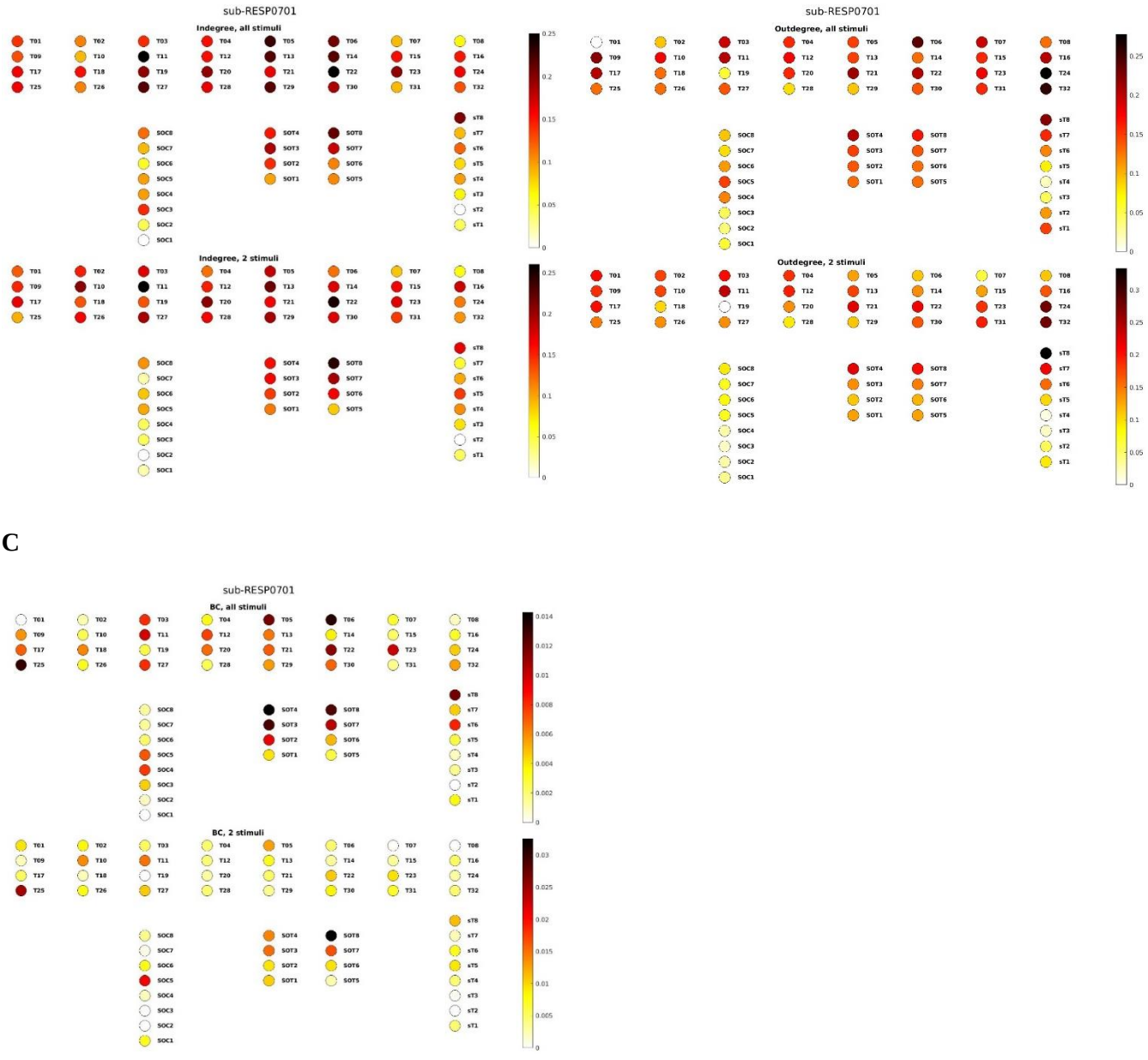


**C**




*Figure A1: 2D grid visualisation of the **A)** in-degree, **B)** out-degree and **C)** betweenness centrality for RESP0701.*

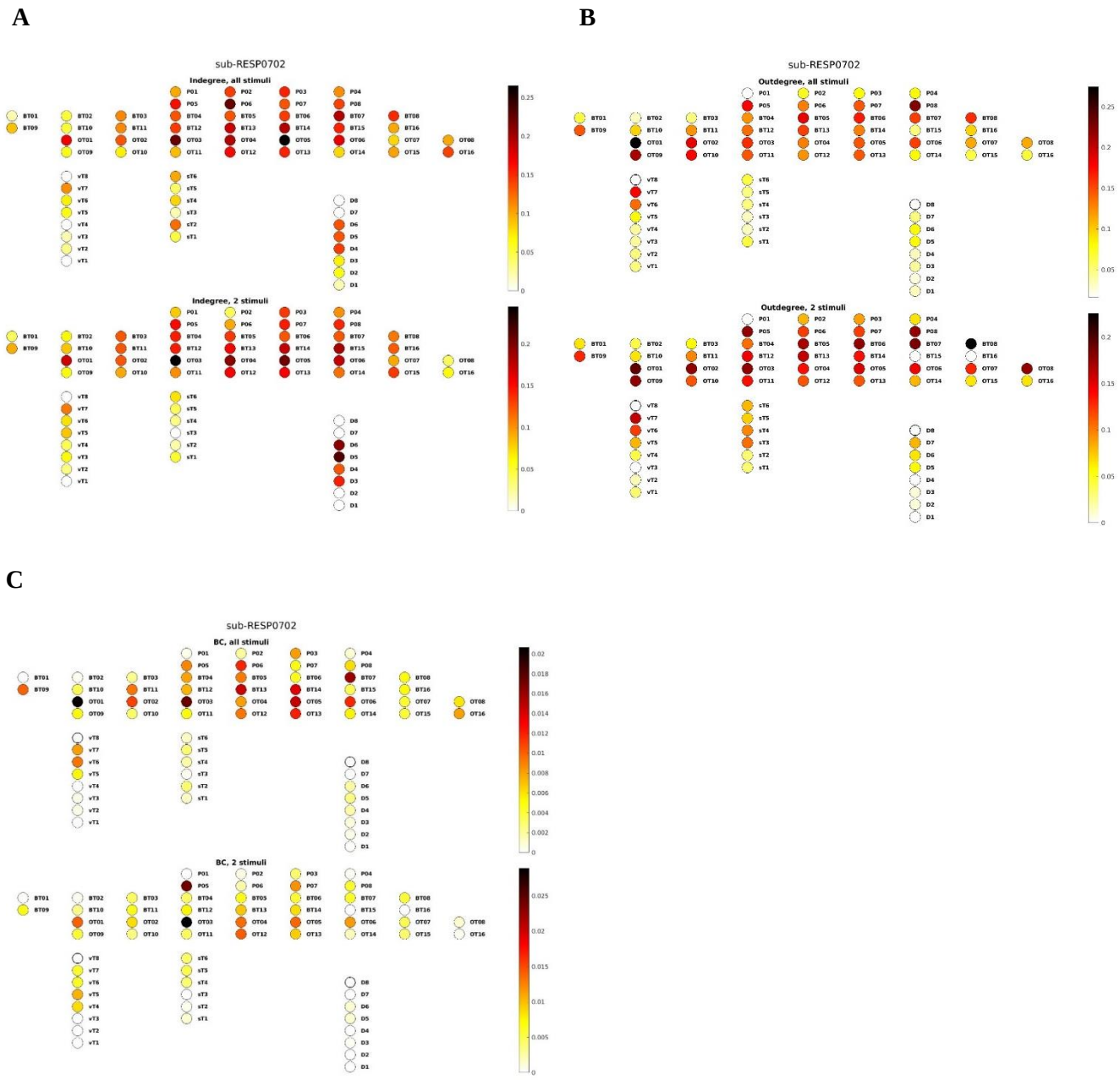


*Figure A2: 2D grid visualisation of the **A)** in-degree, **B)** out-degree and **C)** betweenness centrality for RESP0702.*

**A**

**B**

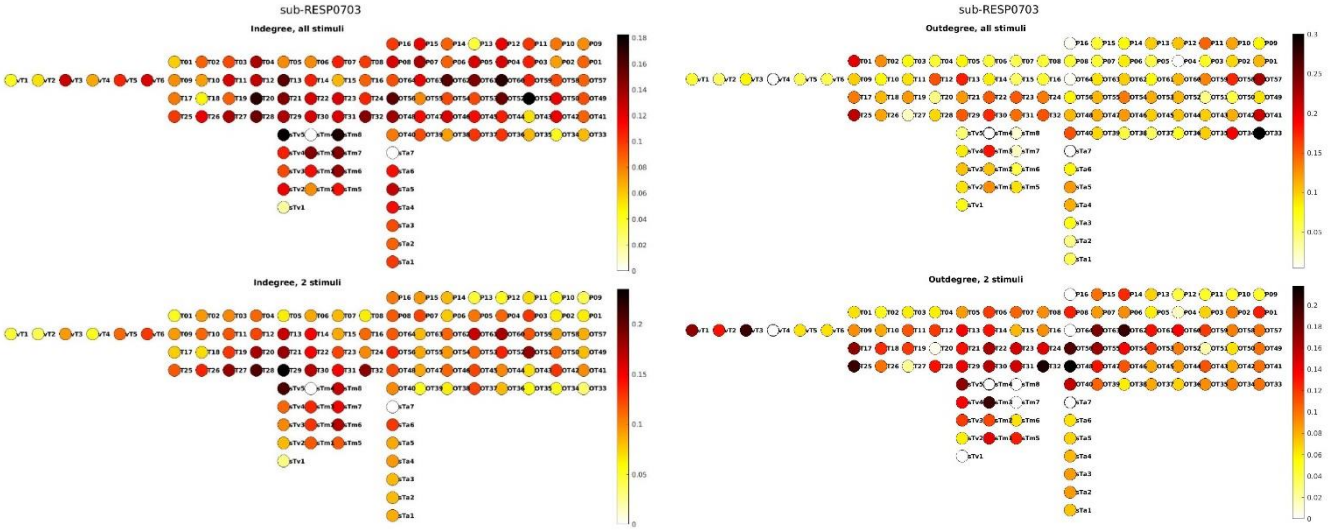


**C**

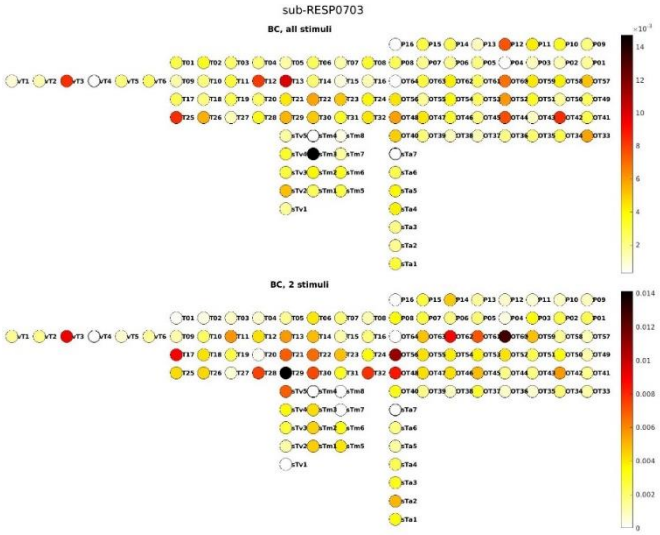


*Figure A3: 2D grid visualisation of the **A)** in-degree, **B)** out-degree and **C)** betweenness centrality for RESP0703.*

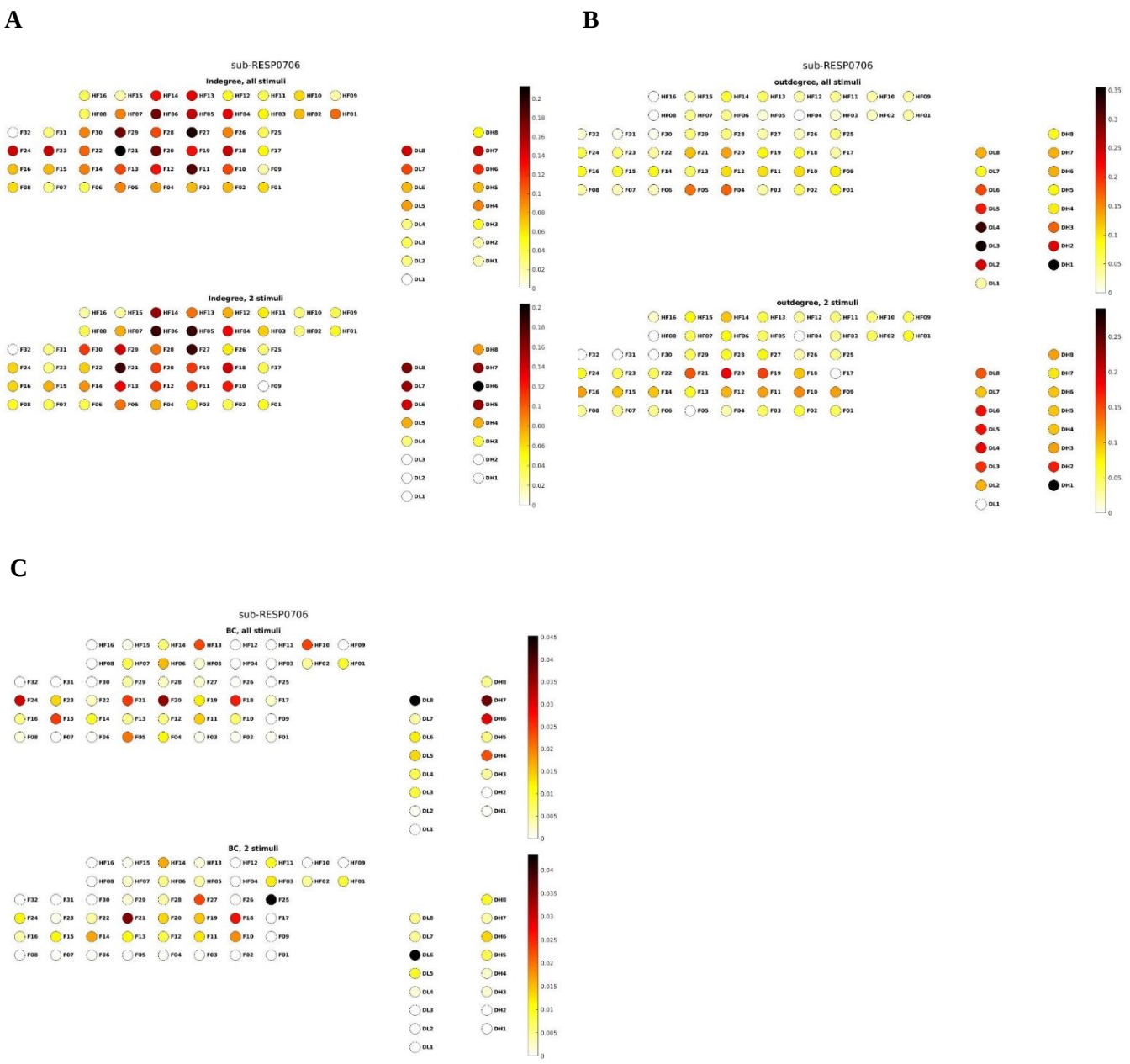


*Figure A4: 2D grid visualisation of the **A)** in-degree, **B)** out-degree and **C)** betweenness centrality for RESP0706.*

**A**

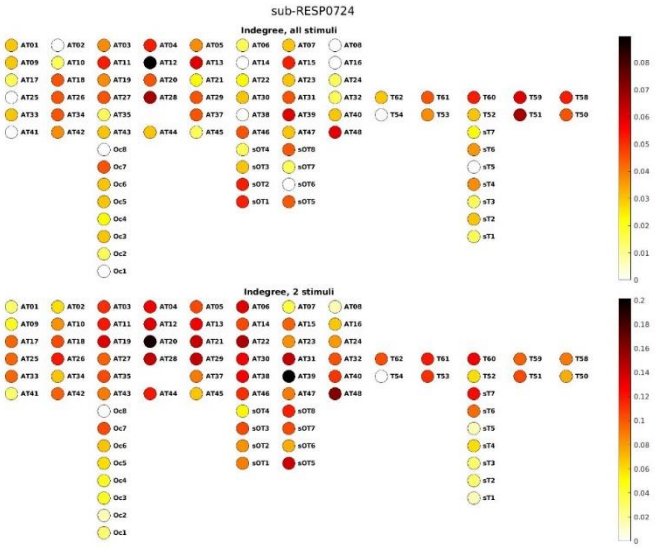


**B**

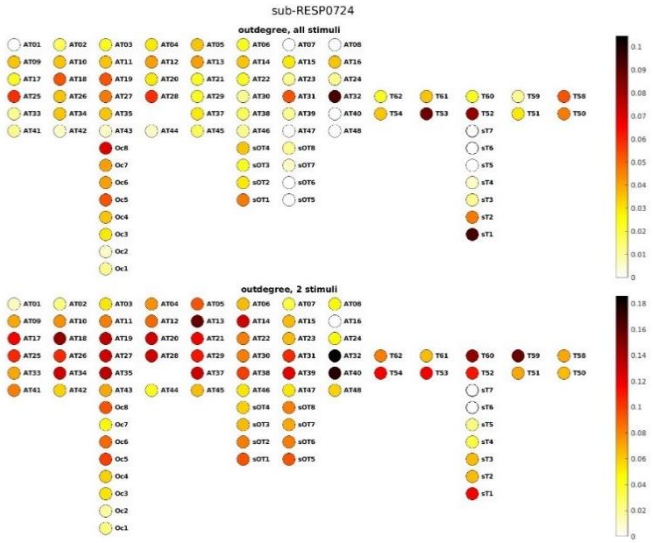


**C**

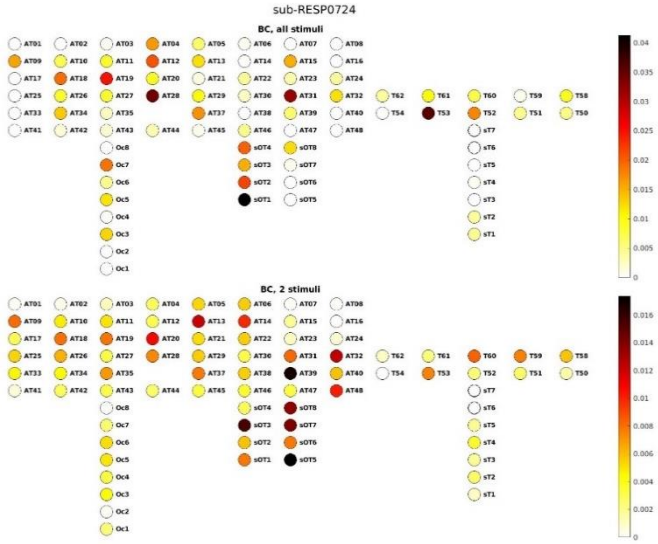


*Figure A5: 2D grid visualisation of the **A)** in-degree, **B)** out-degree and **C)** betweenness centrality for RESP07024.*

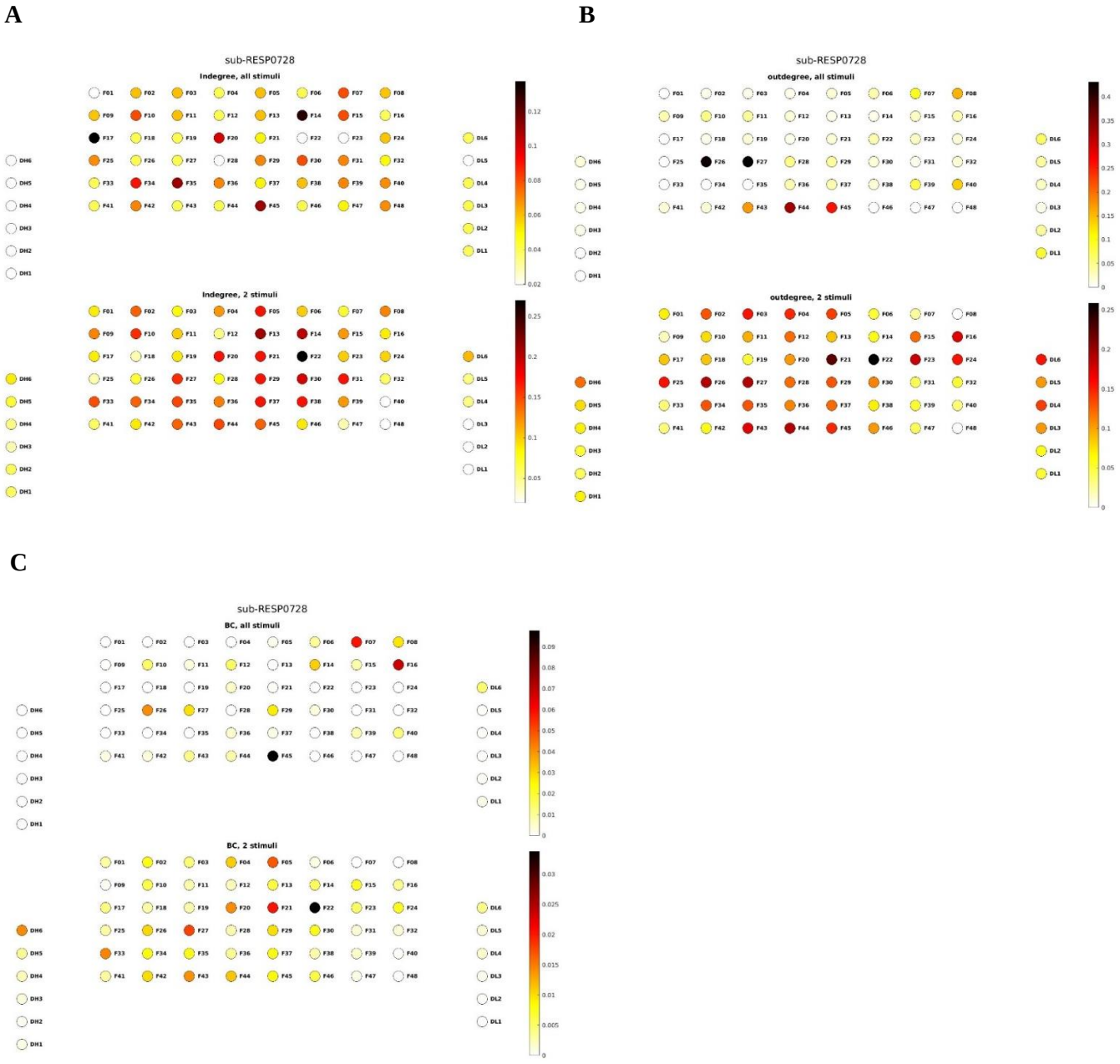


*Figure A6: 2D grid visualisation of the **A)** in-degree, **B)** out-degree and **C)** betweenness centrality for RESP07028.*

# Appendix B:

The 2D grid visualisation of the network characteristics of all patients of the prospective analysis in *Chapter 3.* The SOZ is marked in the green area. Different scales for the colour bar were used to show that the electrodes with the highest value during the clinical-SPES still had the highest value during the propofol-SPES.

**A**

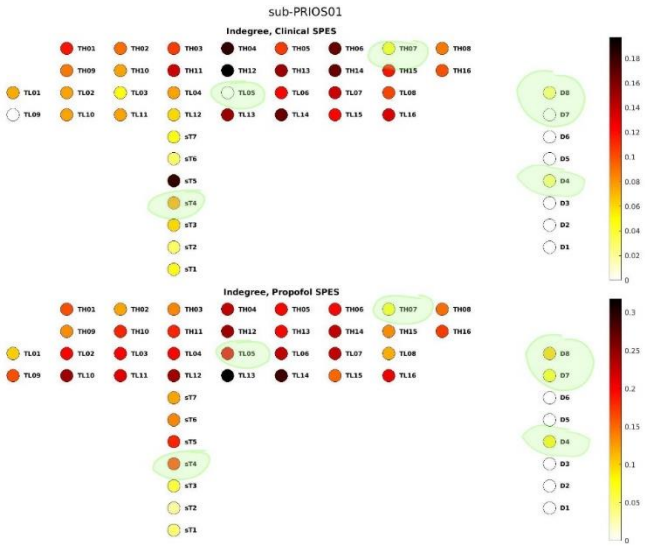


**B**

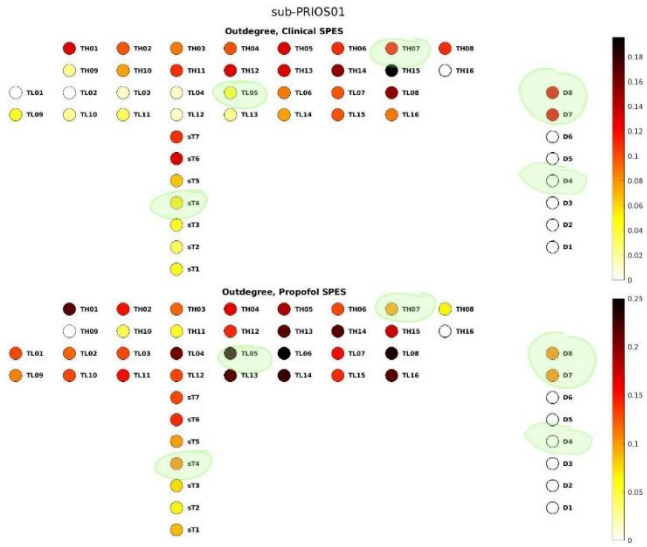


**C**

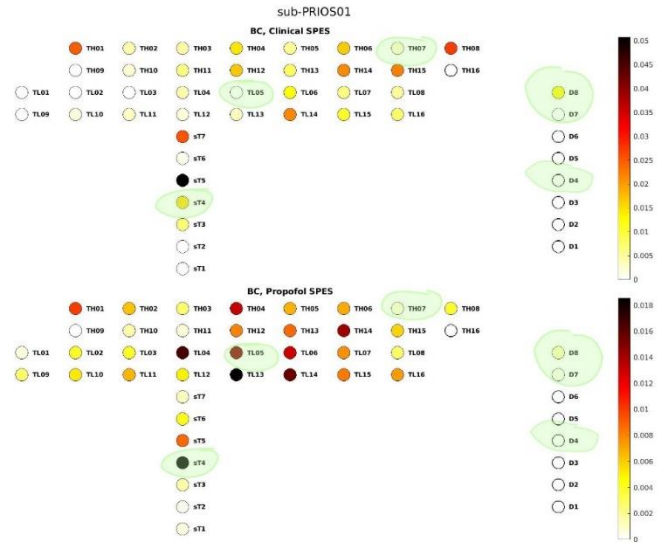


*Figure B1: 2D grid visualisation of the **A)** in-degree, **B)** out-degree and **C)** betweenness centrality for PRIOS01.*

**A**

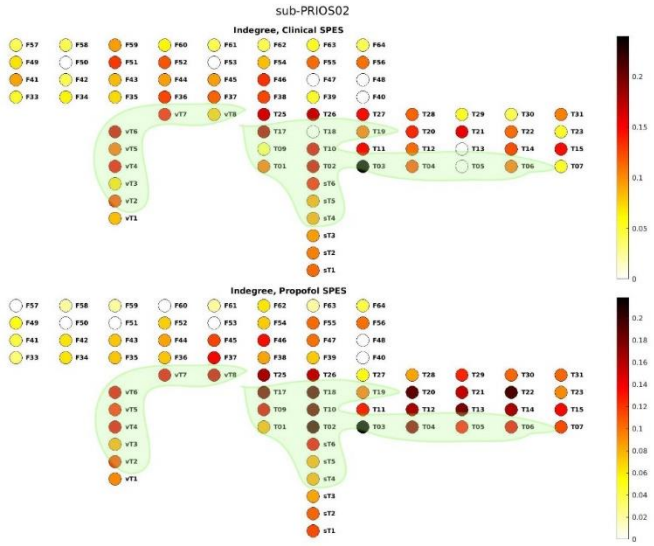


**B**

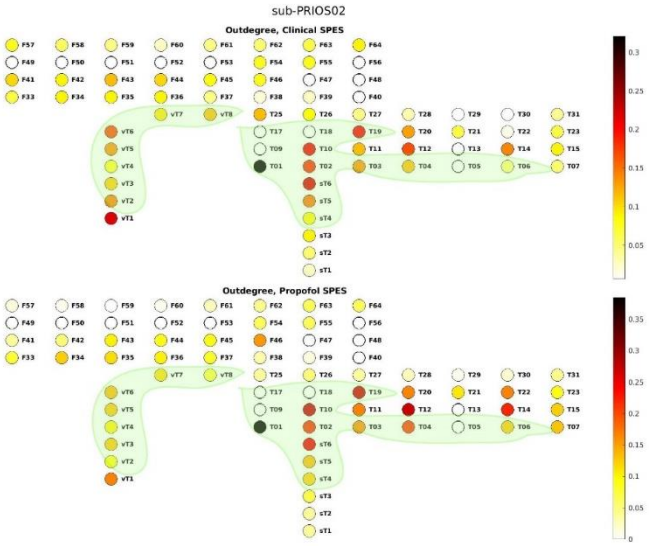


**C**

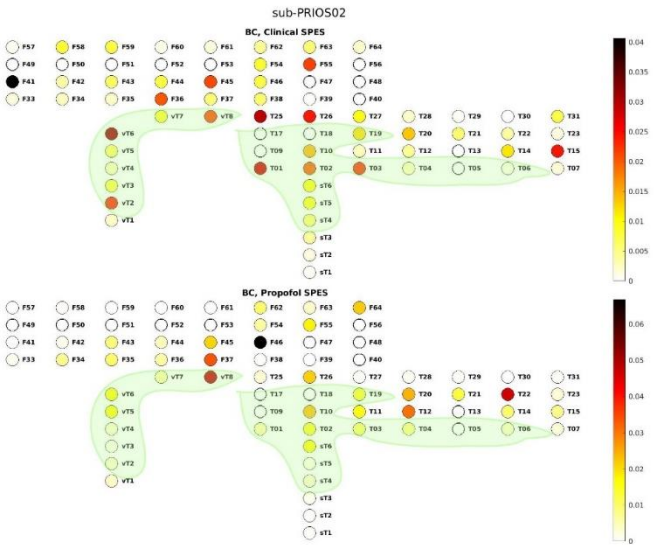


*Figure B2: 2D grid visualisation of the **A)** in-degree, **B)** out-degree and **C)** betweenness centrality for PRIOS02.*

**A**

**B**


**C**

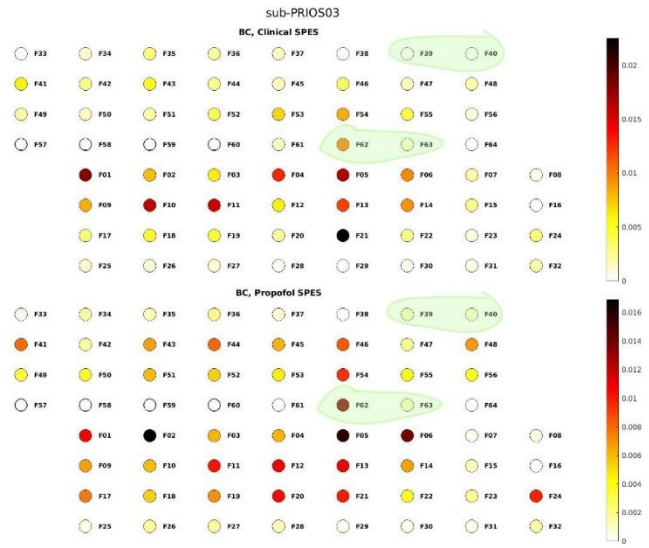


*Figure B3: 2D grid visualisation of the **A)** in-degree, **B)** out-degree and **C)** betweenness centrality for PRIOS03.*

**A**

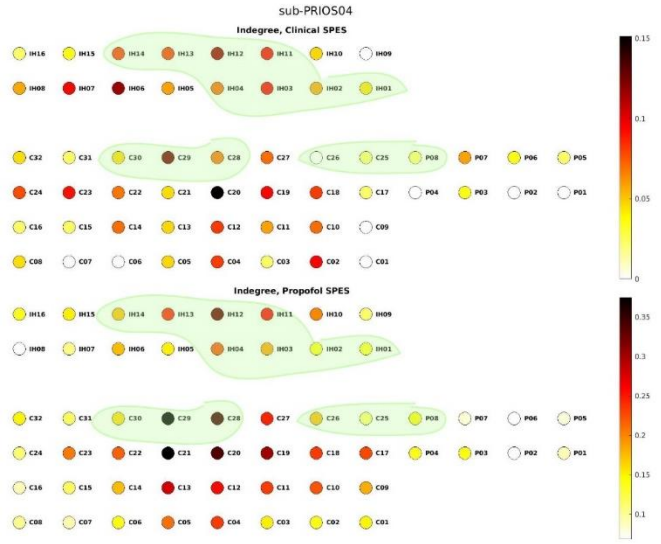


**B**

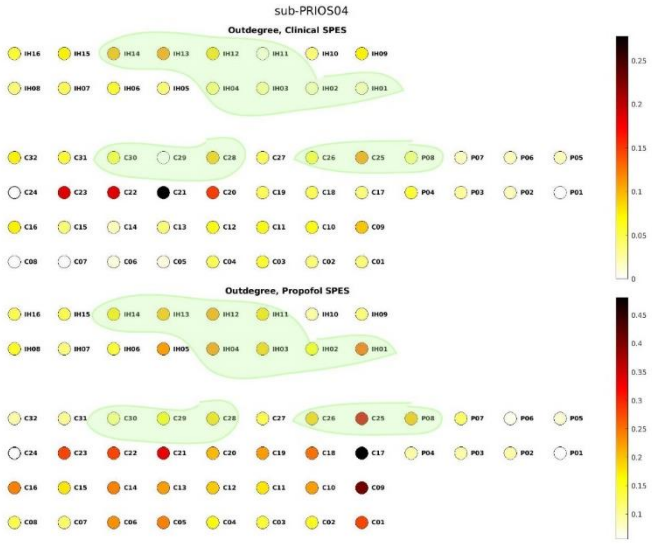


**C**

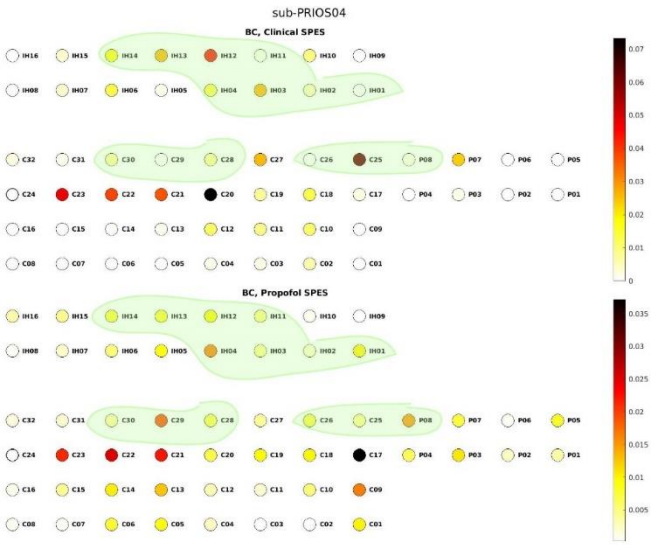


*Figure B4: 2D grid visualisation of the **A)** in-degree, **B)** out-degree and **C)** betweenness centrality for PRIOS04.*

**A**

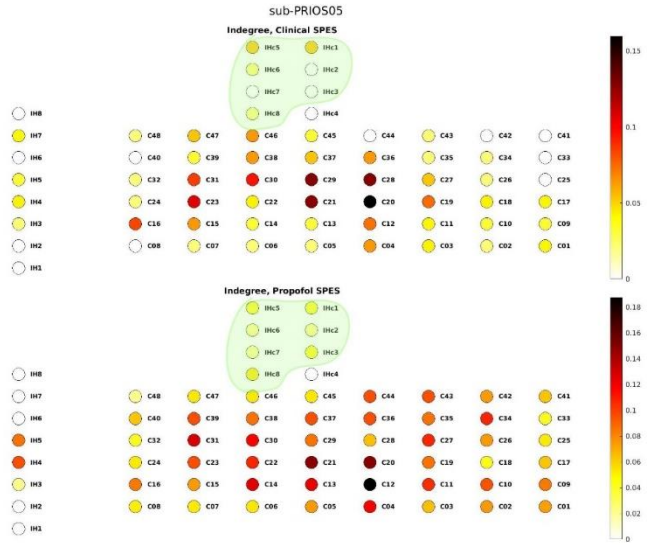


**B**

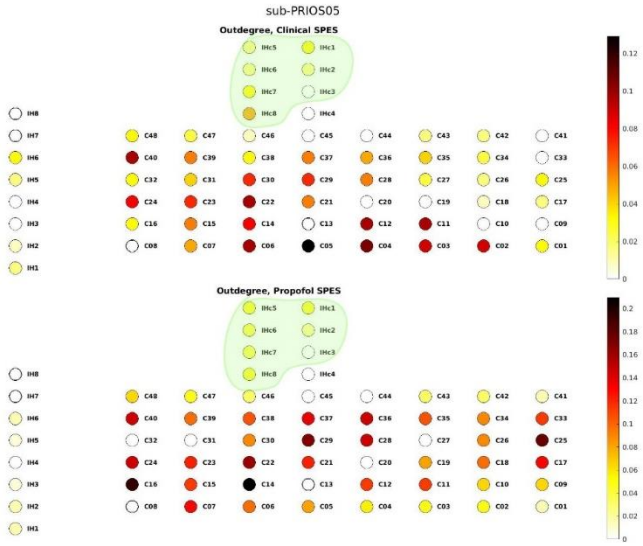


**C**

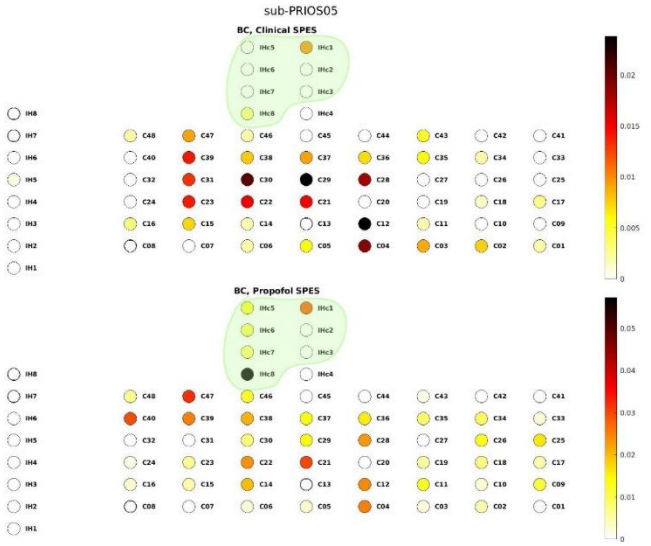


*Figure B5: 2D grid visualisation of the **A)** in-degree, **B)** out-degree and **C)** betweenness centrality for PRIOS05.*

**A**

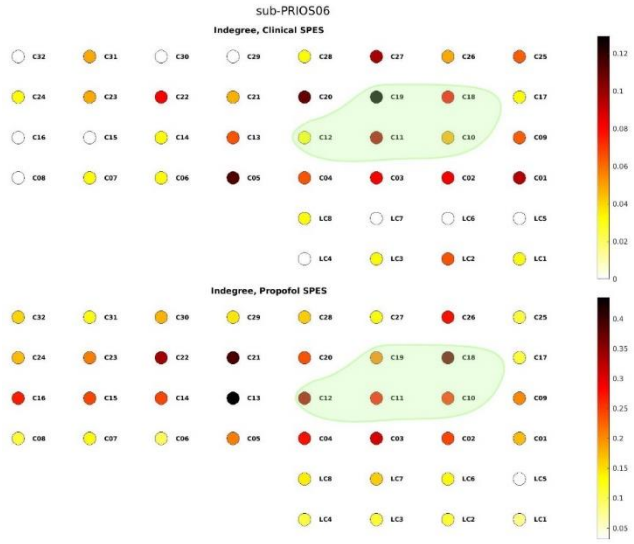


**B**


**C**

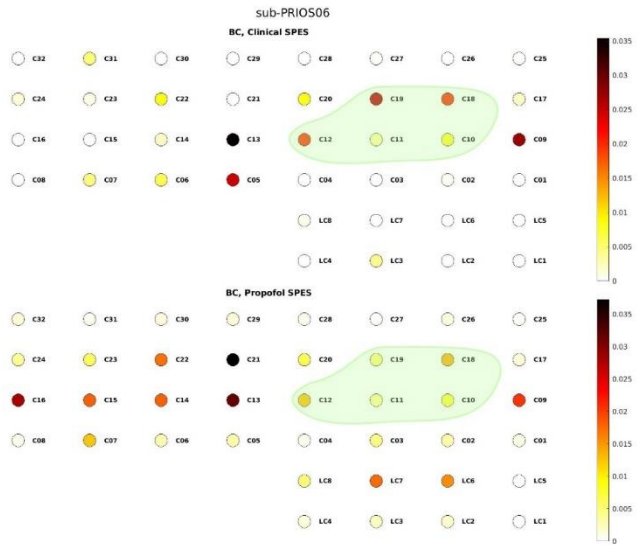


*Figure B6: 2D grid visualisation of the **A)** in-degree, **B)** out-degree and **C)** betweenness centrality for PRIOS06.*

# Appendix C:

Examples of in vivo responses to stimuli during the clinical-SPES and propofol-SPES for each patient. The response of the clinical-SPES is an average of 10 stimuli, the response of the propofol-SPES is an average of at least 2 stimuli.

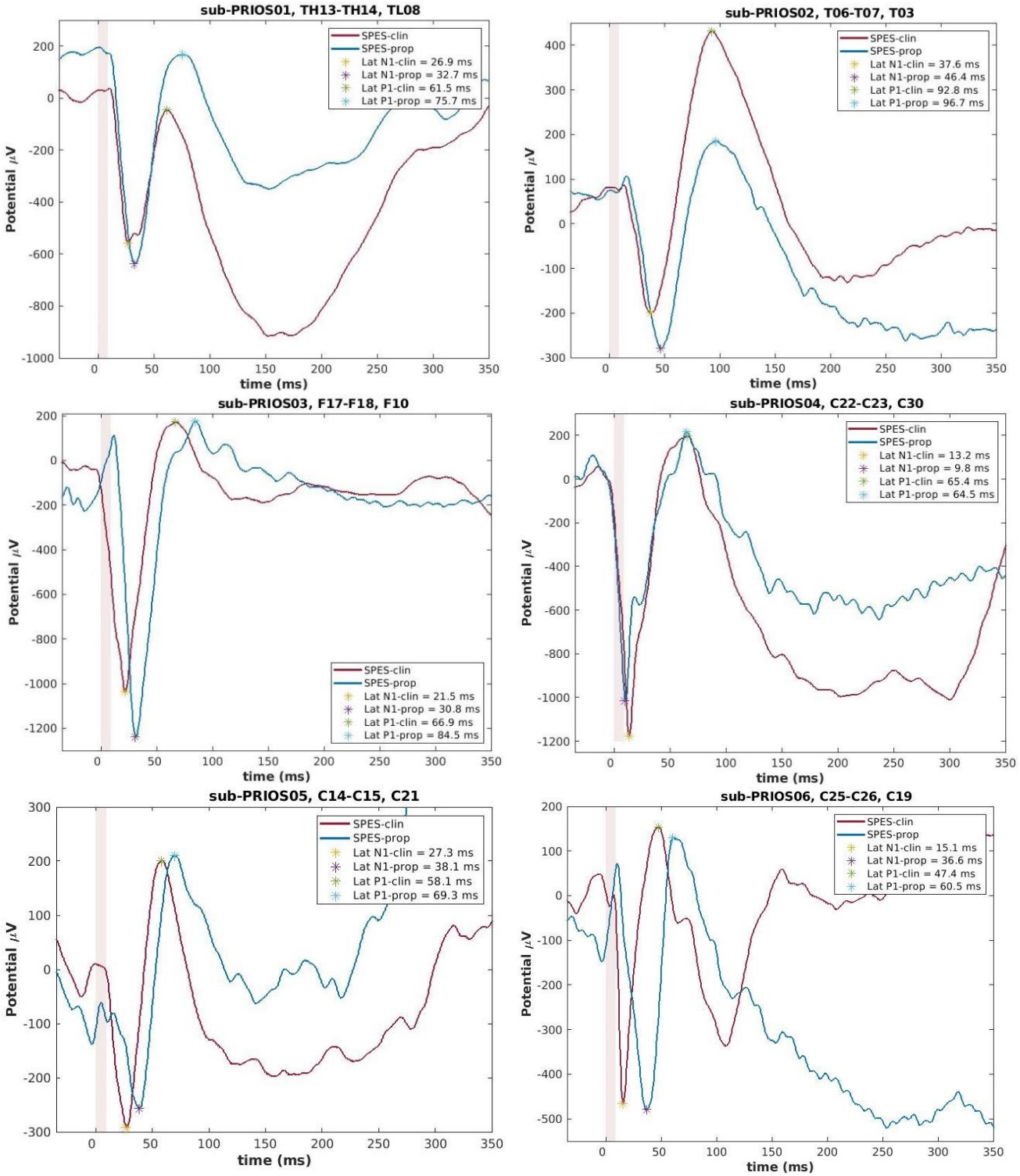


*Figure C.1: In red the averaged response of a clinical-SPES stimulus, in blue the average response on the same electrode-stimulation pair combination for the propofol-SPES. The legend provides the latency (in ms) for the N1- and P1-peak. The orange patch is the interval [-1.5 ms: 9ms] where interpolation is used around the stimulation artefact.*

**The latency of the N1-, P1- and N2-peaks**

Violin plots in *Figure C.2* show that the median N1-latency during propofol-SPES increased for PRIOS02, PRIOS03, PRIOS04 and PRIOS05. The median P1-latency during propofol-SPES increased for all patients except PRIOS06. The N2-latency was only determined for PRIOS03. The N2-latency increased significantly.

**A**

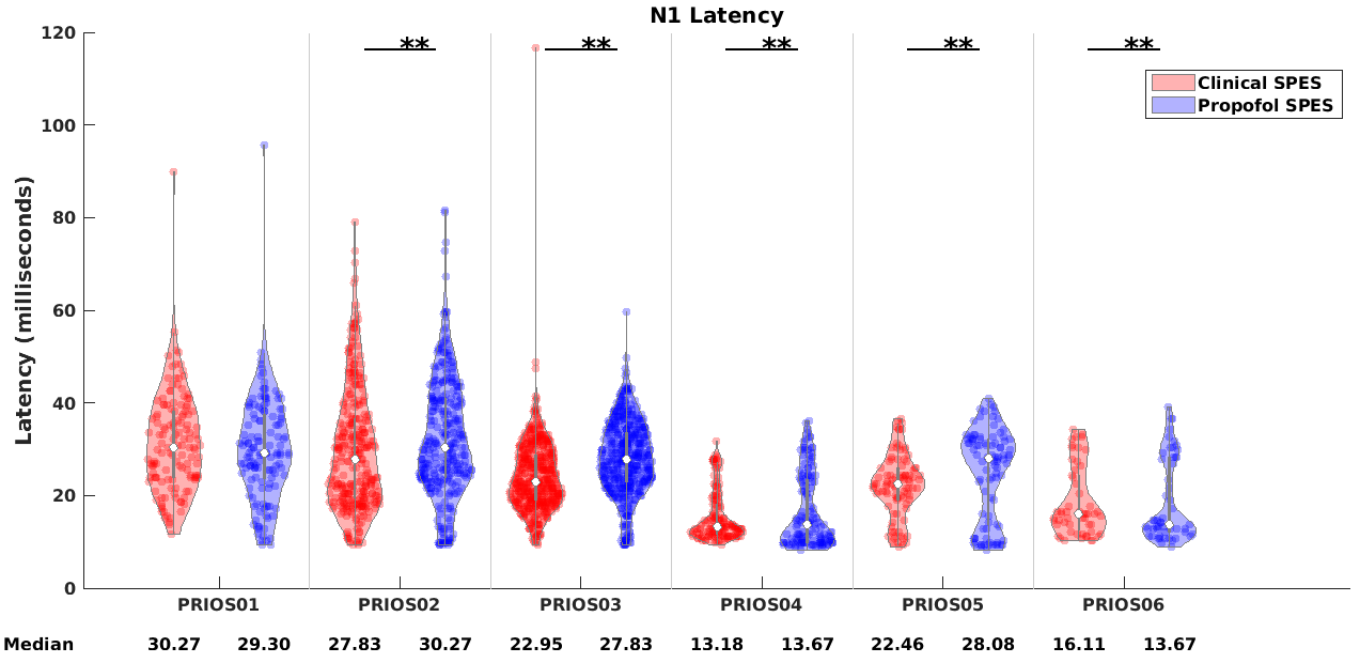


*Figure continues on next page*

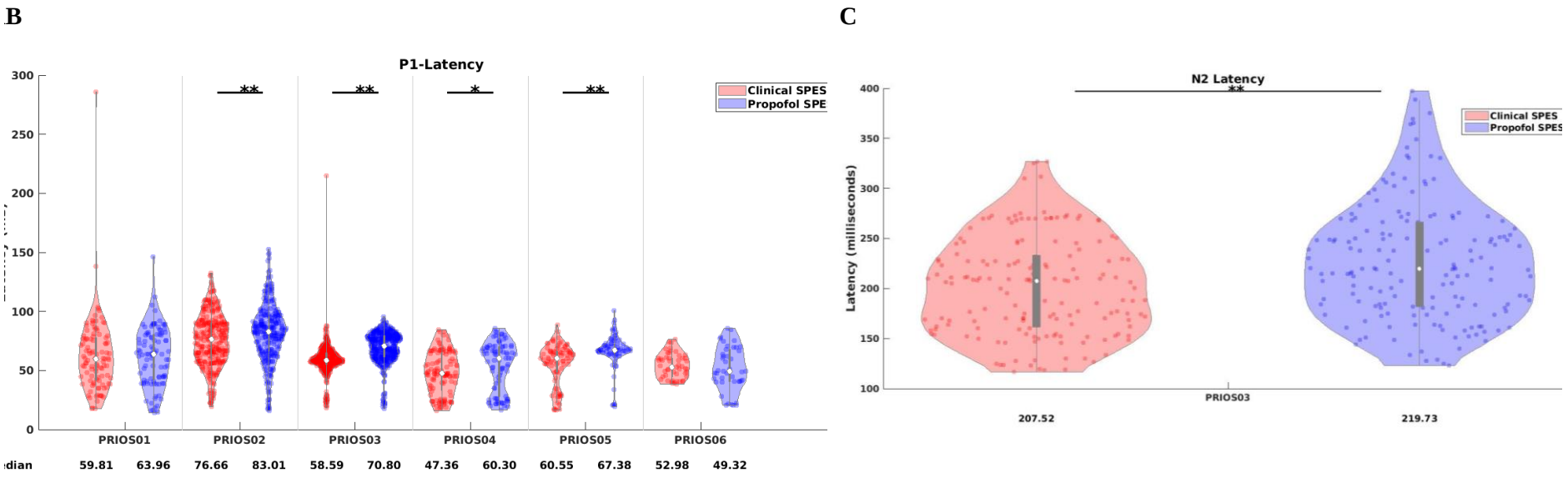


*Figure C.2:* ***A&B)*** *The N1- and the P1-latency in ms. In red the clinical-SPES and in blue the propofol-SPES for all six patients.* ***C)*** *The N2-latency of PRIOS03. The median value is provided below each violin plot. (** indicates p<0.001, * indicates p<0.05).*

# Appendix D:

**Modelling SPES responses**

We used an extended Wendling model as described by *Hebbink et al. (2020)* [35], [37]. This included the four populations (i.e. pyramidal, excitatory, fast and slow inhibitory) and feedforward inhibition. Each population has a mean membrane potential, that is influenced by other populations or external inputs via synaptic transmissions. These synaptic transmissions convert the mean activity/firing rate ($z$) of the sending population into a postsynaptic potential (PSP) at the receiving population. This PSP is modelled by a linear, second-order differential equation:

$$\ddot{x}(t) = Qqz(t) - 2q\dot{x}(t) - q^2x(t) \tag{D.1}$$

The differential equation is characterised by an impulse response *h:*

$$h(t) = \begin{cases} Qqte^{-qt} & t \geq 0 \\ 0 & t < 0 \end{cases} \tag{D.2}$$

in which $Q$ is the synaptic gain that regulates that magnitude, and $1/q$ is the rising time of the synapse. The rising time is the time after which the impulse response reaches its maximum.

A sigmoid function converts the mean membrane potential to a mean firing rate ($z$) from the sending population. This indicates that the firing rate will saturate when reaching a certain mean membrane potential. We used the sigmoid settings described by *Hebbink et al. (2020)* [35], [37].

*Table D1: Parameters and their default value of the neural mass model to simulate SPES* [35], [37]. *Adapted default values are indicated in the second column in orange.*

| **Para-meter** | **Description** | **Default value *Hebbink et al. (2020)*** | **Default values used in this study** |
|---|---|---|---|
| $A$ | Excitatory synaptic gain | 4.5 mV | 4.5 mV |
| $B$ | Slow inhibitory synaptic gain | 7 mV | 7 mV |
| $G$ | Fast inhibitory synaptic gain | 25 mV | 25 mV |
| $a$ | Reciprocal of the excitatory time constant | 100 $s^{-1}$ | 100 $s^{-1}$ |
| $b$ | Reciprocal of the slow inhibitory time constant | 10 $s^{-1}$ | **4.6 $s^{-1}$** |
| $g$ | Reciprocal of the fast inhibitory time constant | 300 $s^{-1}$ | 300 $s^{-1}$ |
| $\beta$ | Scaling constant external input to the slow inhibitory | 1 | 1 |
| $\gamma$ | Scaling constant external input to the fast inhibitory | 0.7 | 0.7 |
| $c_1$ | Relative conn. strength from pyramidal to excitatory | 1 | 1 |
| $c_2$ | Relative conn. strength from excitatory to pyramidal | 0.8 | 0.8 |
| $c_3$ | Relative conn. strength from pyramidal to slow inhibitory | 0.25 | 0.25 |
| $c_4$ | Relative conn. strength from slow inhibitory to pyramidal | 0.25 | 0.25 |
| $c_5$ | Relative conn. strength from pyramidal to fast inhibitory | 0.3 | 0.3 |
| $c_6$ | Relative conn. strength from slow to fast inhibitory | 0.1 | 0.1 |
| $c_7$ | Relative conn. strength from fast inhibitory to pyramidal | 0.8 | 0.8 |

Each population has its own parameter for $Q$ and $q$. The default values, of *Hebbink et al. (2020)* [35], [37], are provided in *Table D1*. This results in the following set of differential equations that model the PSP of the four populations and for external input (SPES):

$$\ddot{x}_{py}(t) = AaS(u_{py}) - 2a\dot{x}_{py}(t) - a^2 x_{py}(t) \quad \text{(D.3)}$$

$$\ddot{x}_{ex}(t) = AaS(u_{ex}) - 2a\dot{x}_{ex}(t) - a^2 x_{ex}(t) \quad \text{(D.4)}$$

$$\ddot{x}_{is}(t) = BbS(u_{is}) - 2b\dot{x}_{is}(t) - b^2 x_{is}(t) \quad \text{(D.5)}$$

$$\ddot{x}_{if}(t) = GgS(u_{if}) - 2g\dot{x}_{if}(t) - g^2 x_{if}(t) \quad \text{(D.6)}$$

$$\ddot{x}_{SPES}(t) = AaI - 2a\dot{x}_{SPES}(t) - a^2 x_{SPES}(t) \quad \text{(D.7)}$$

Using the default settings results in the impulse responses of the uncoupled populations as shown in *Figure D1*.

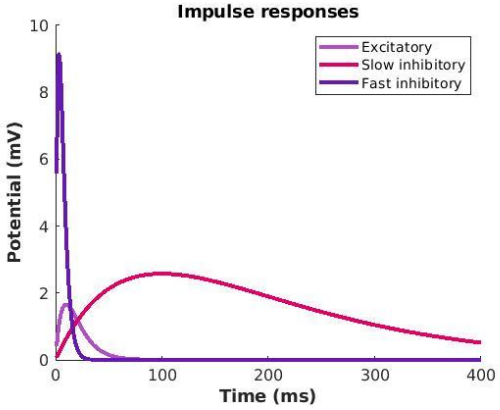


*Figure D1: Impulse responses of the excitatory, slow inhibitory and fast inhibitory populations as a function of time.*

The equations for the mean membrane potentials of the populations are given by *Equation D.8 – D.11*. $C_1$ to $C_7$ are the relative connectivity strength between the populations, see *Figure D2*. The default settings are provided in *Table D1*.

$$u_{py} = C_2 x_{ex} - C_4 x_{is} - C_7 x_{if} + x_{SPES} \quad \text{(D.8)}$$

$$u_{ex} = C_1 x_{py} \quad \text{(D.9)}$$

$$u_{is} = C_3 x_{py} + \beta x_{SPES} \quad \text{(D.10)}$$

$$u_{if} = C_5 x_{py} + C_6 x_{si} + \gamma x_{SPES} \quad \text{(D.11)}$$

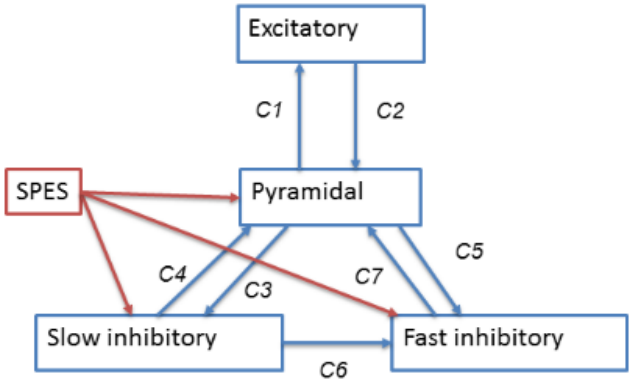


*Figure D2: Architecture of a single neural mass with the pyramidal population in the centre, surrounded by the excitatory population, the slow inhibitory population and the fast inhibitory population. SPES is represented here as an external input (red arrows). The blue arrows represent connections between the populations with their connection strength parameters* $C_n$ [35], [37].

**Decrease of the gain and time constant of the fast inhibitory population**

Decreasing the time constant $(g)$ for the fast inhibitory population, led to an increase in the latency of the N1-, P1- and N2-peak, see *Figure D4.3*. It can also be seen that reducing the time constant did not influence the N2-latency for values $G < 21\,mV$. None of the settings results in an unstable response, see *Figure D4.3d*.

**A**

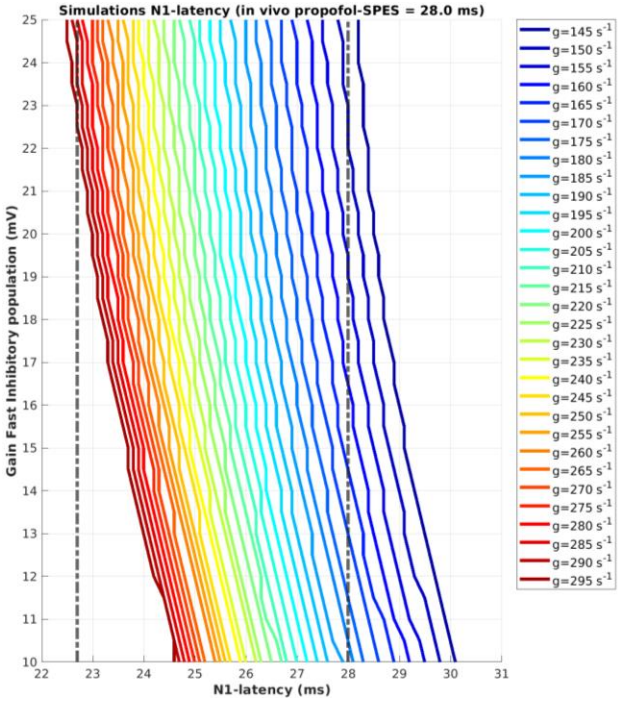


**B**

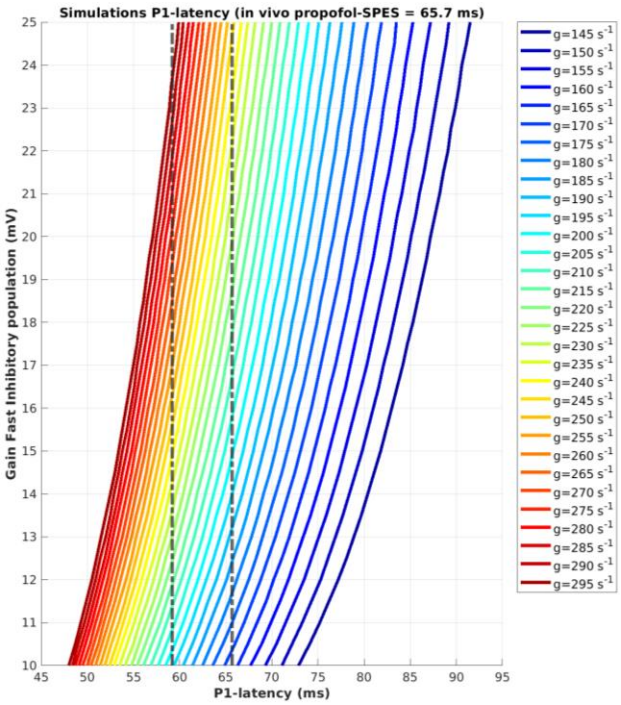


*Figure continues on next page*

**C** **D**

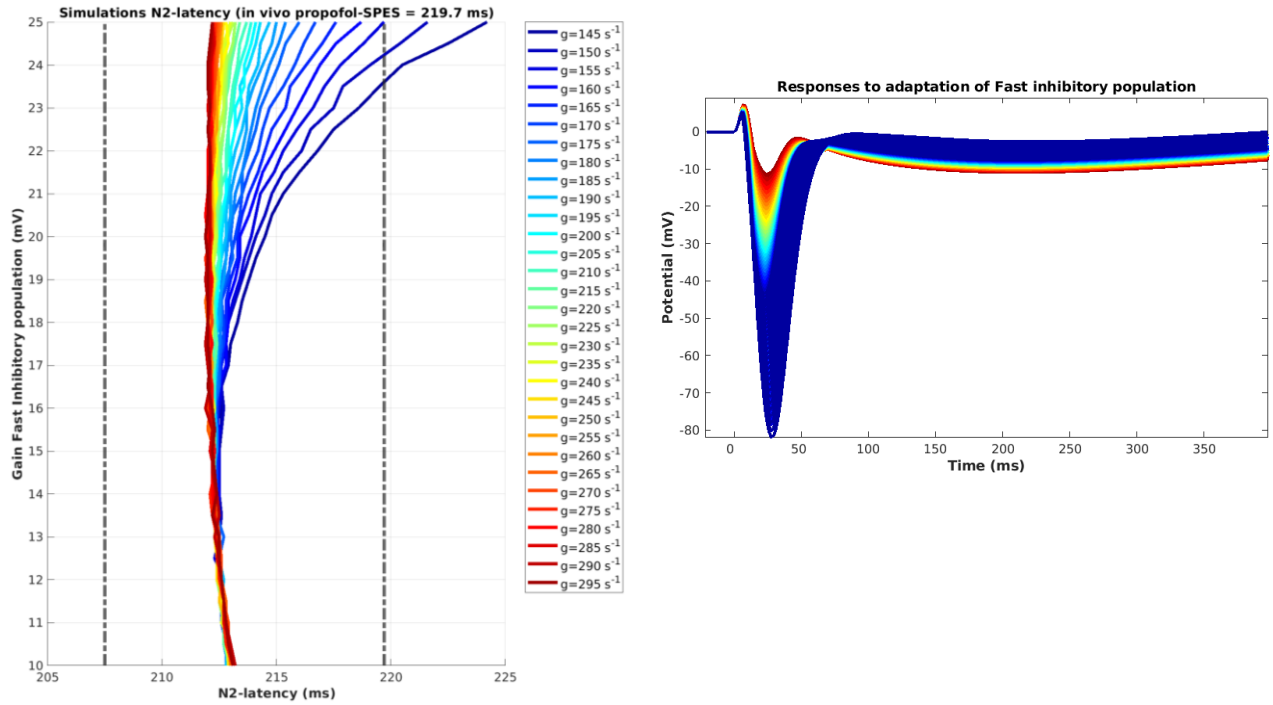


*Figure D3: A) the latency results for the N1-peak, B) the latency results for the P1-peak, C) the latency results for the N2-peak. The x-axis of A, B&C represents the latency in $ms$, the y-axis represents the value for the gain of the fast inhibitory population $(G)$ in $mV$ and the different colour lines represent the time constant of the fast inhibitory population $(g)$ in $s^{-1}$ with the values provided in the legend. The dashed line on the left represents the median N1/P1/N2-latency found during our in vivo clinical-SPES, the dashed line on the right represents the median N1/P1/N2-latency found during our in vivo propofol-SPES. D) The plot of all responses, none of the settings results in an unstable response.*